



NMDB Meeting 2025: Cosmic Ray studies with Neutron Detectors
Athens, 19 – 21 March 2025

*Shape and extend of the Heliosphere and Cosmic
Ray Modulation and solar wind transition surfaces
Solar Alfven and Sonic surfaces*

George Exarchos 1 Xenophon Moussas 2

1 Siemens, Athens, Greece

2 National and Kapodistrian University of Athens,

+306978792891 xmoussas@phys.uoa.gr, xdmoussas@gmail.com

copyright: © X MOUSSAS, G EXARHOS and University of Athens 2025

Shape and extend of the solar wind transition surfaces

Solar Alfvén and Sonic surfaces

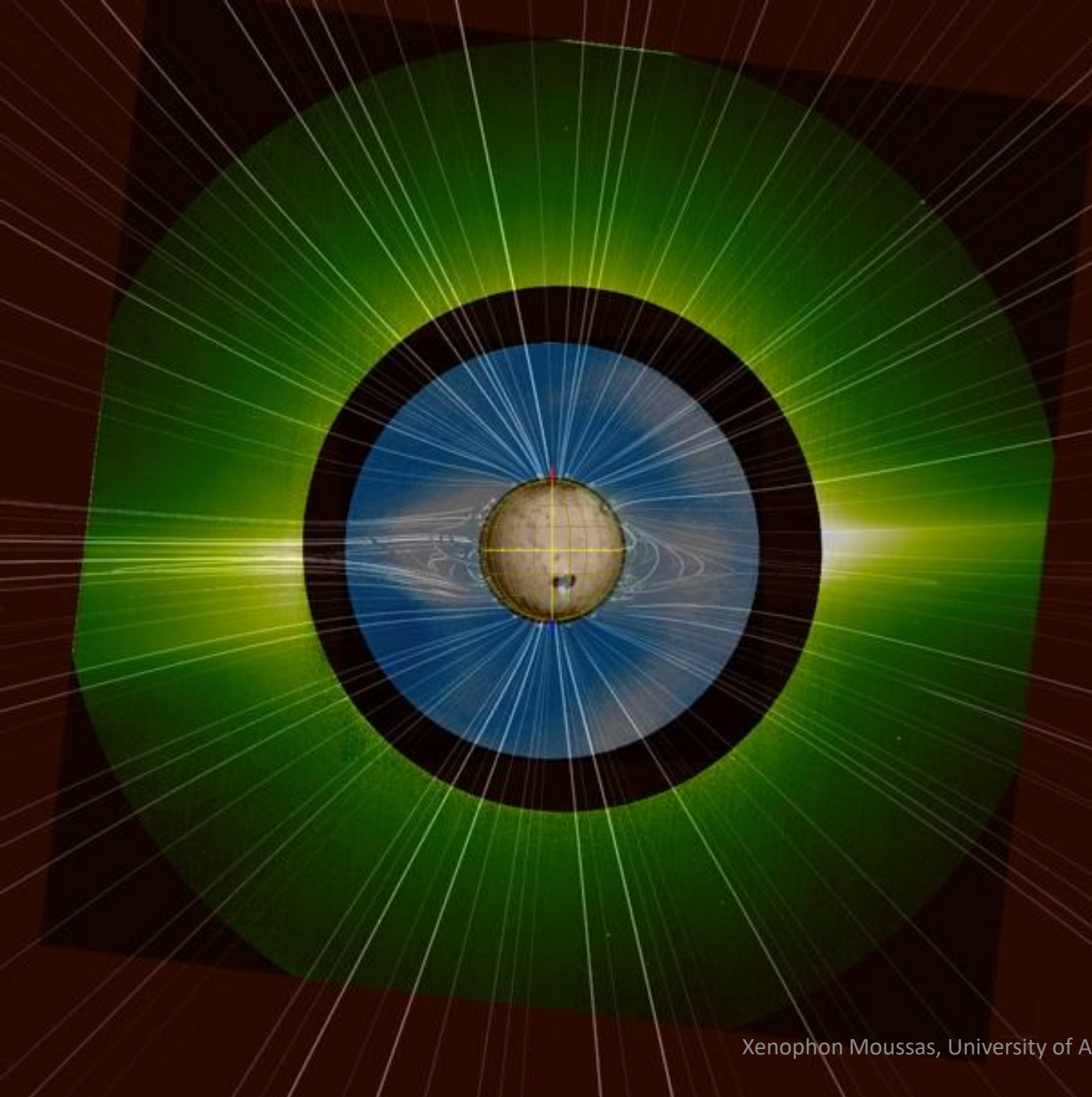
Xenophon Moussas 1 & George Exarchos 2

1 National and Kapodistrian University of Athens,

2 Siemens, Athens, Greece

+306978792891 xmoussas@phys.uoa.gr, xdmoussas@gmail.com



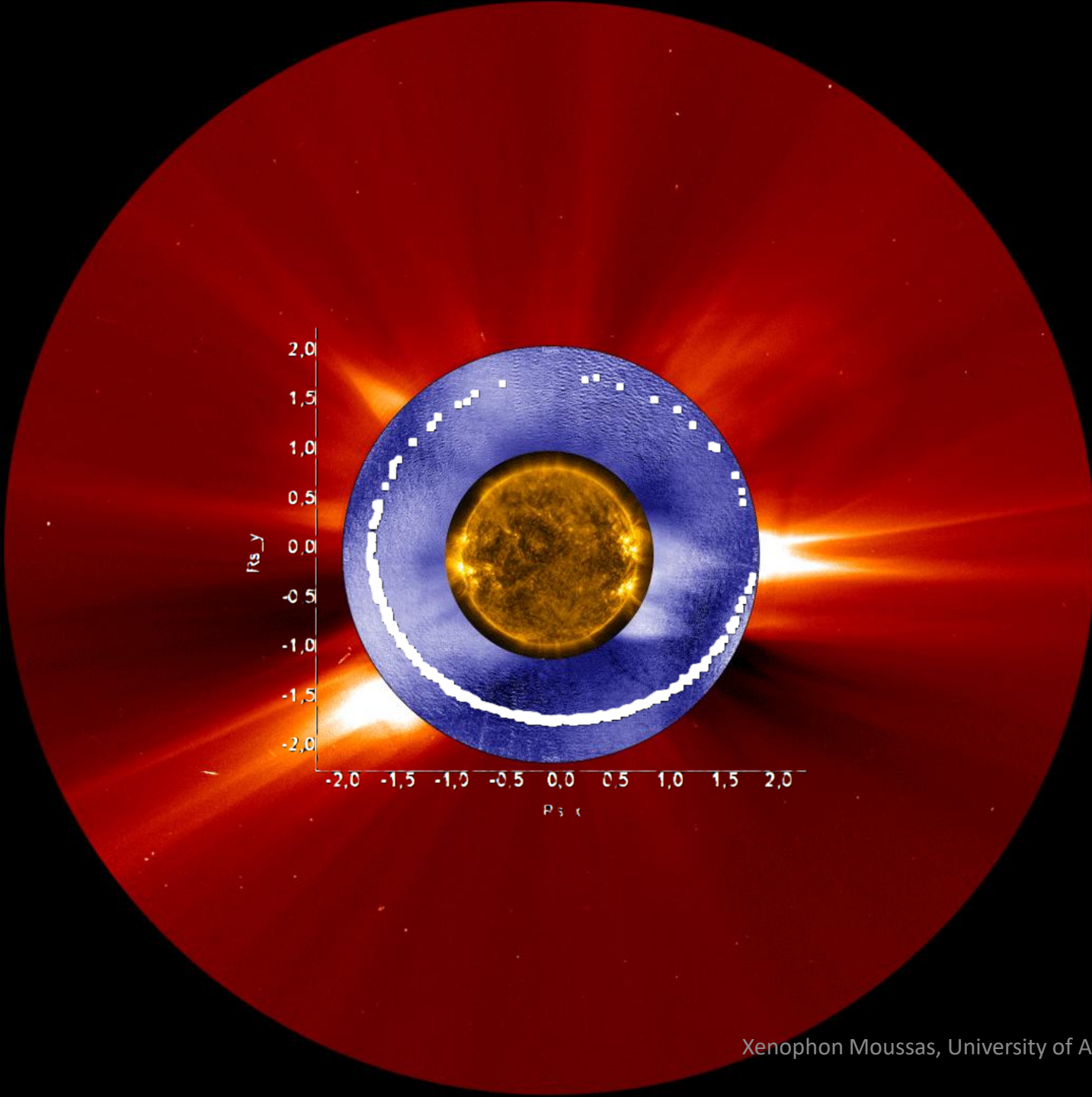


CREDIT

data NSSDCA, PSP OMNI

Solar Orbiter/Metis Team/
ESA & NASA; Mauna Loa
Solar

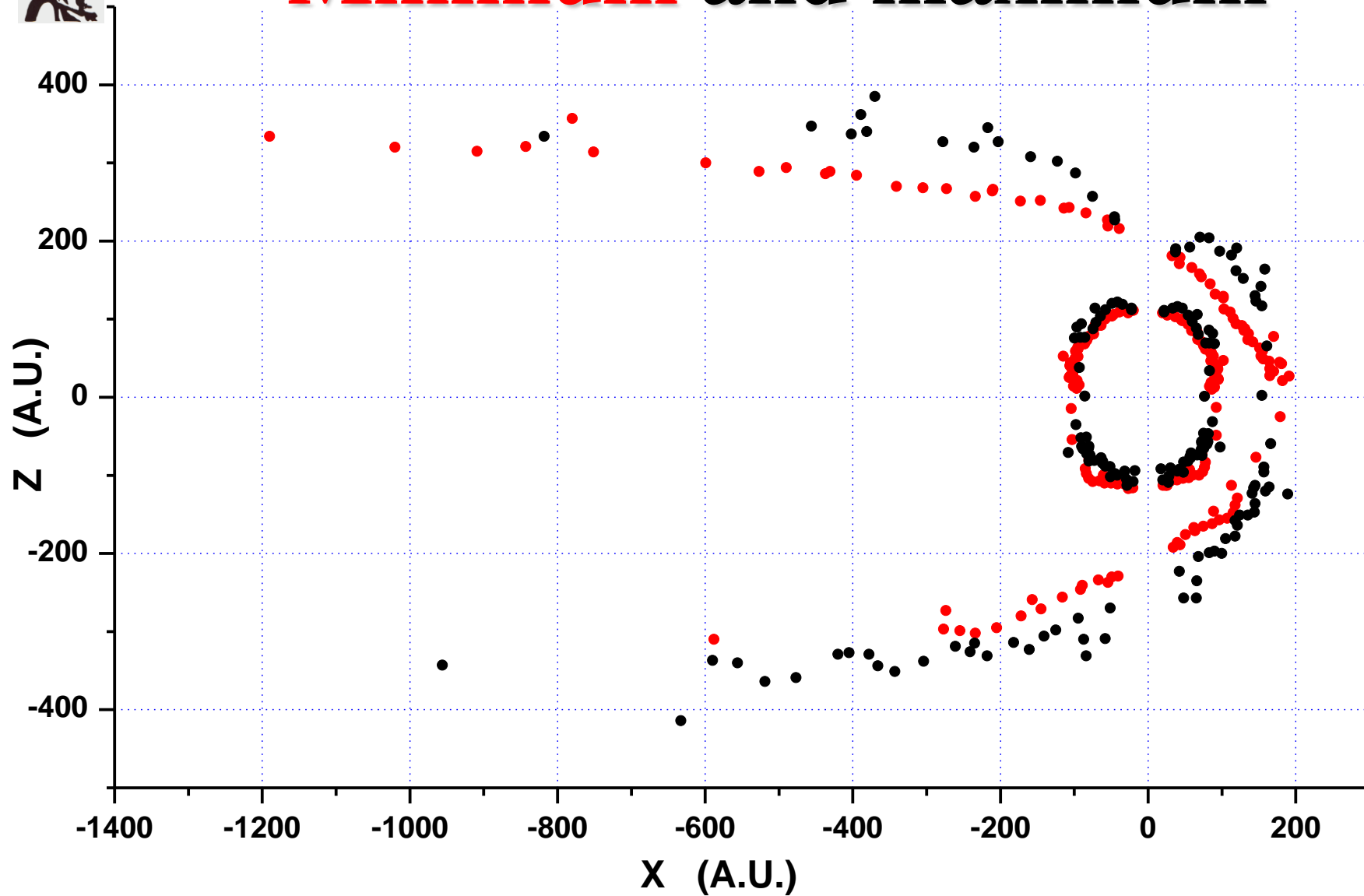
Observatory/HAO/NaCAR
/NSF; Predictive Science
Inc./NASA/NSF/AFOSR;
NASA/SDO/AIA



credit: NASA/ESA/SOHO/SDO/Joy Ng
and MLSO/K-Cor)



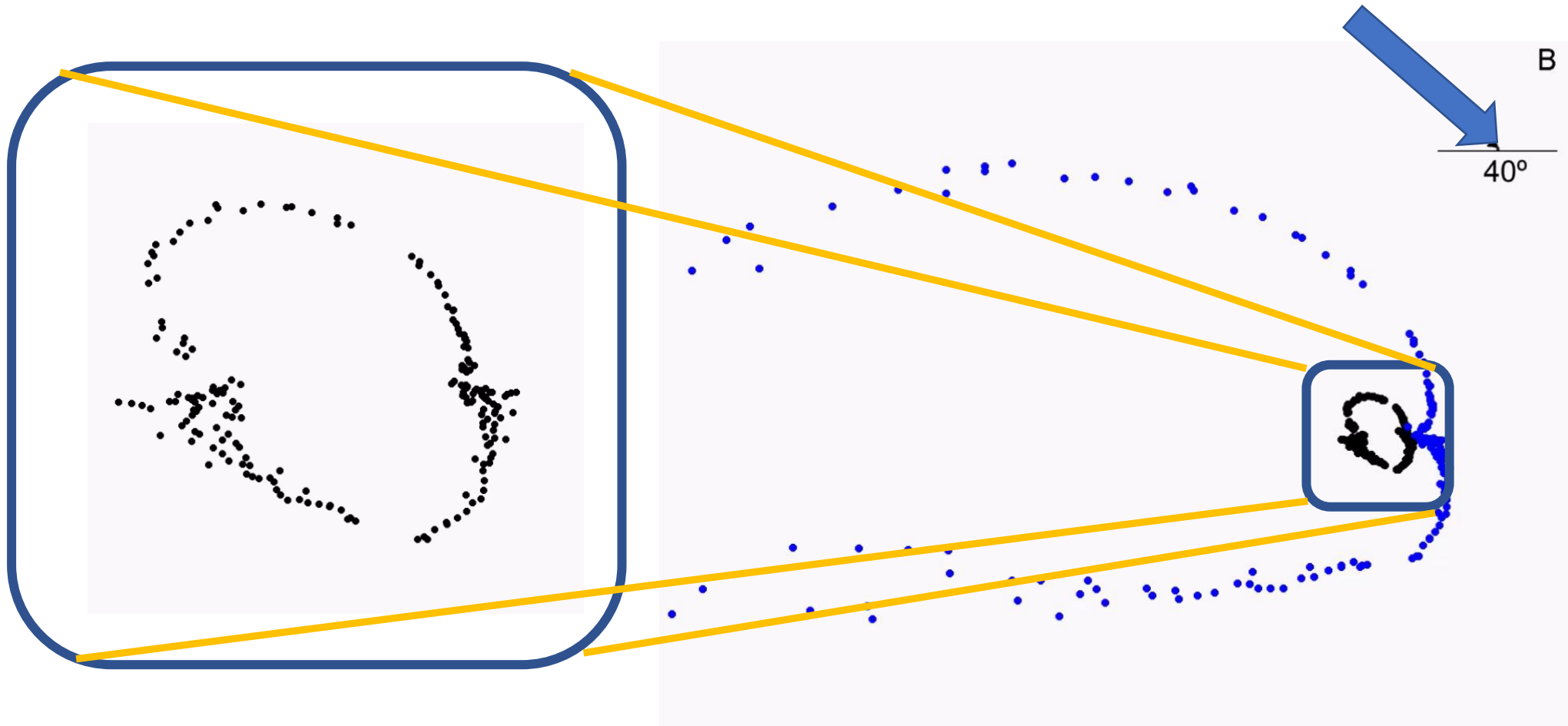
Minimum and maximum

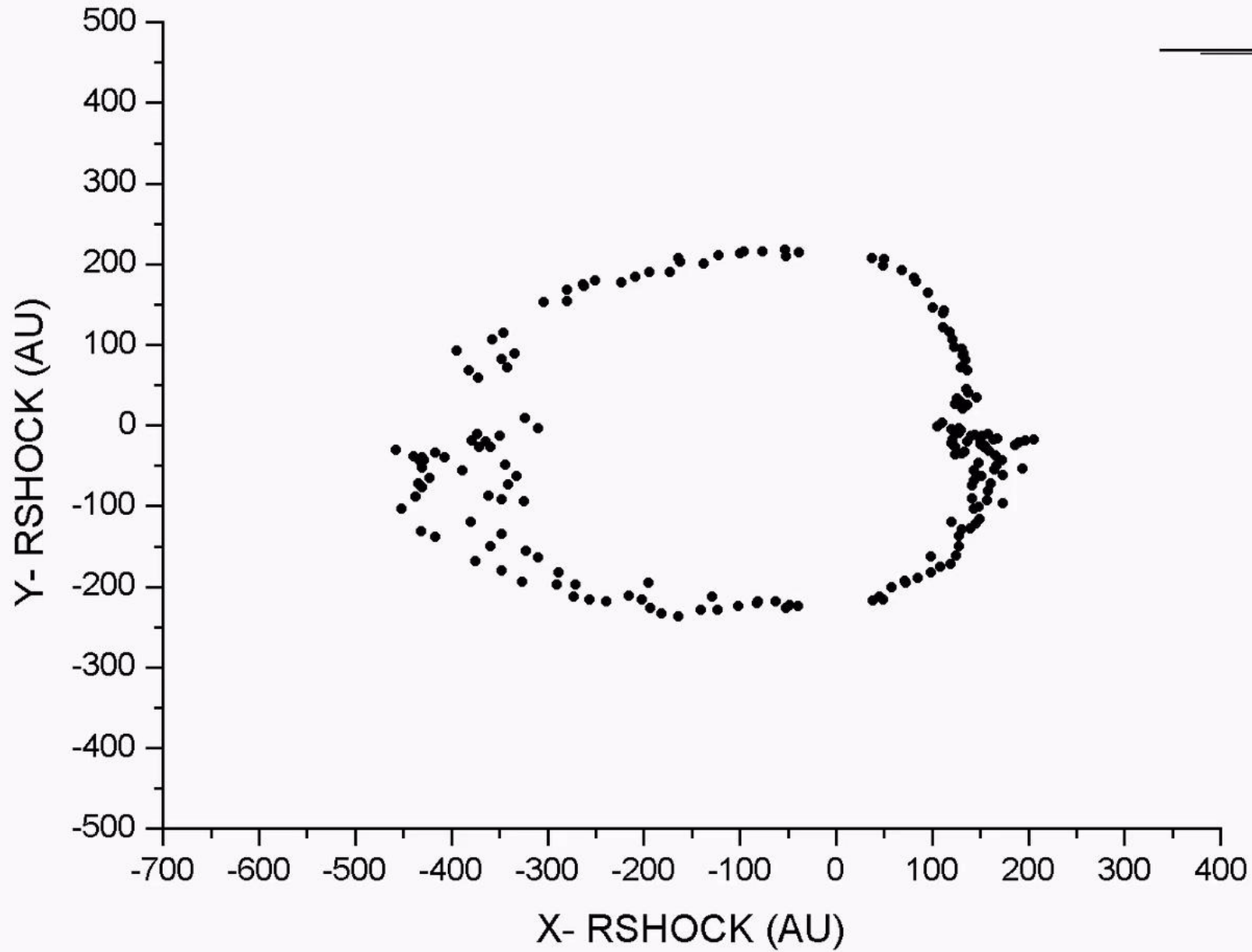


• Days-mean = 27
Period: 1994 - 1997.5
Solar minimum

• Days-mean = 27
Period: 1999.5 - 2002.5
Solar maximum

Shape and extend dependence upon LISM magnetic field direction (~ 2000)





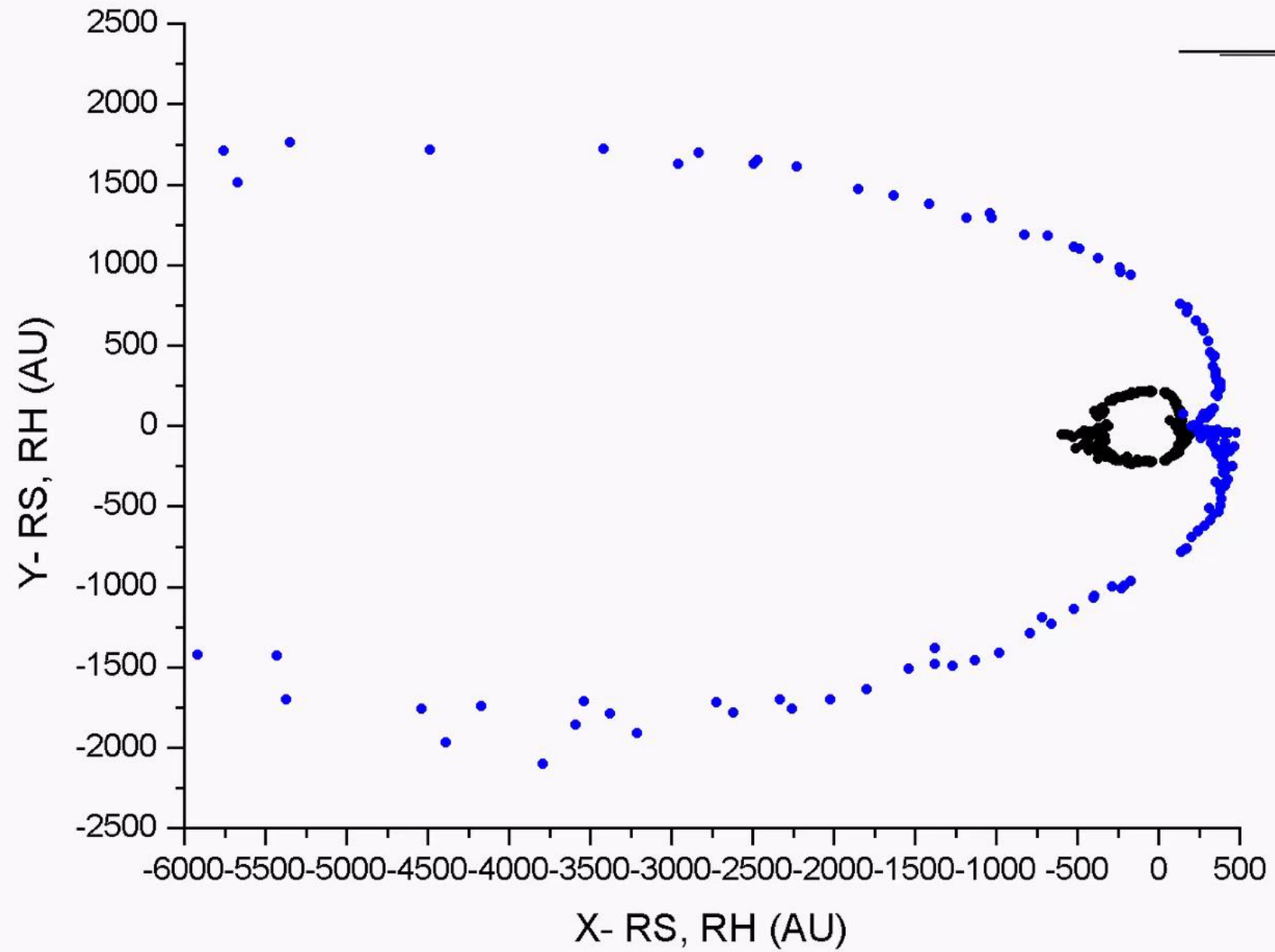
B



George Exarchos
Angeliki Nikolopoulou
Xenophon Moussas
National and Kapodistrian
University of Athens, 2001



B



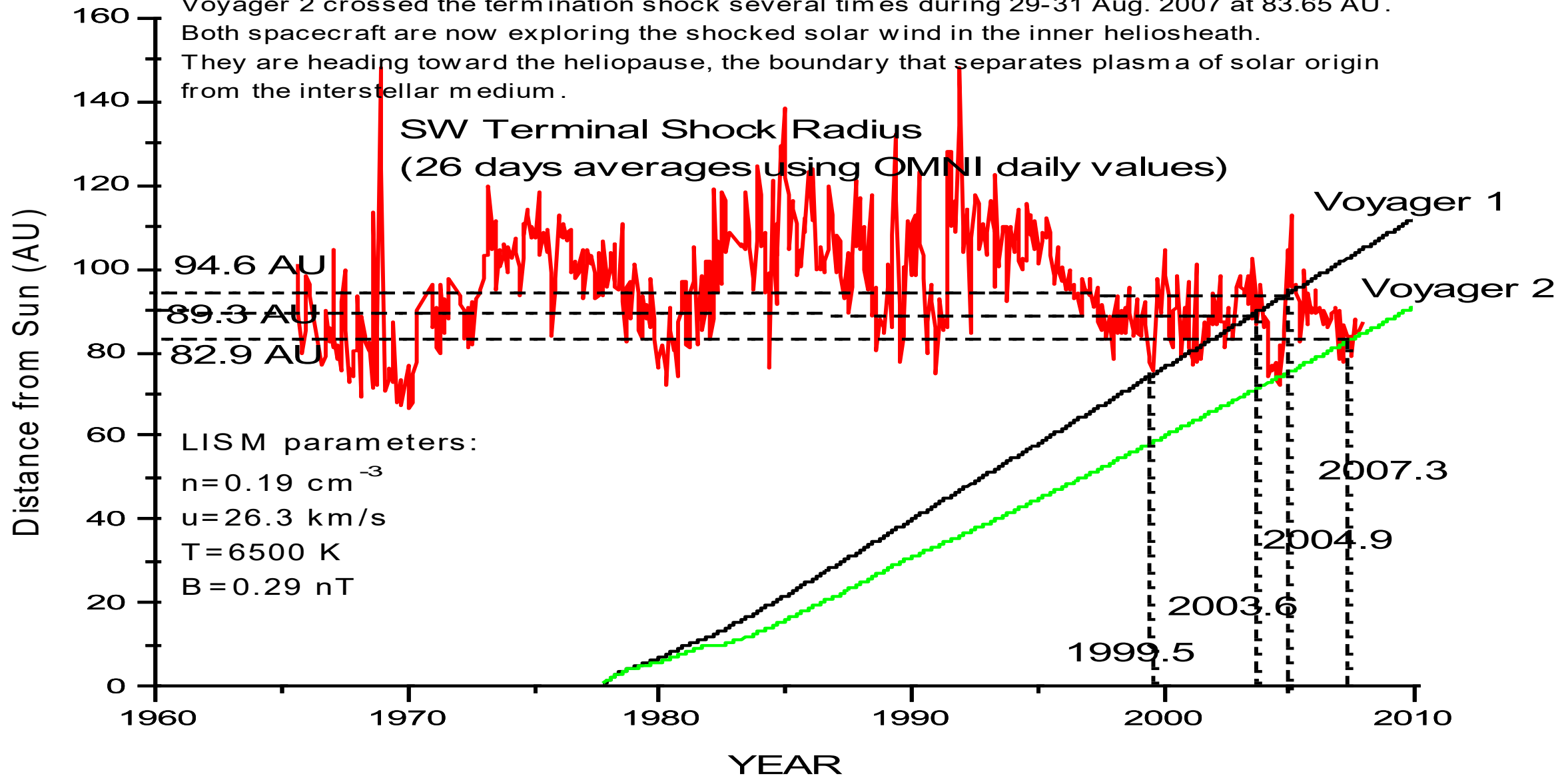
George Exarchos
Angeliki Nikolopoulou
Xenophon Moussas
National and Kapodisrtrian
University of Athens, 2001

Voyager 1 crossed the termination shock of the solar wind on 16 Dec. 2004 at 94.0 AU.

Voyager 2 crossed the termination shock several times during 29-31 Aug. 2007 at 83.65 AU.

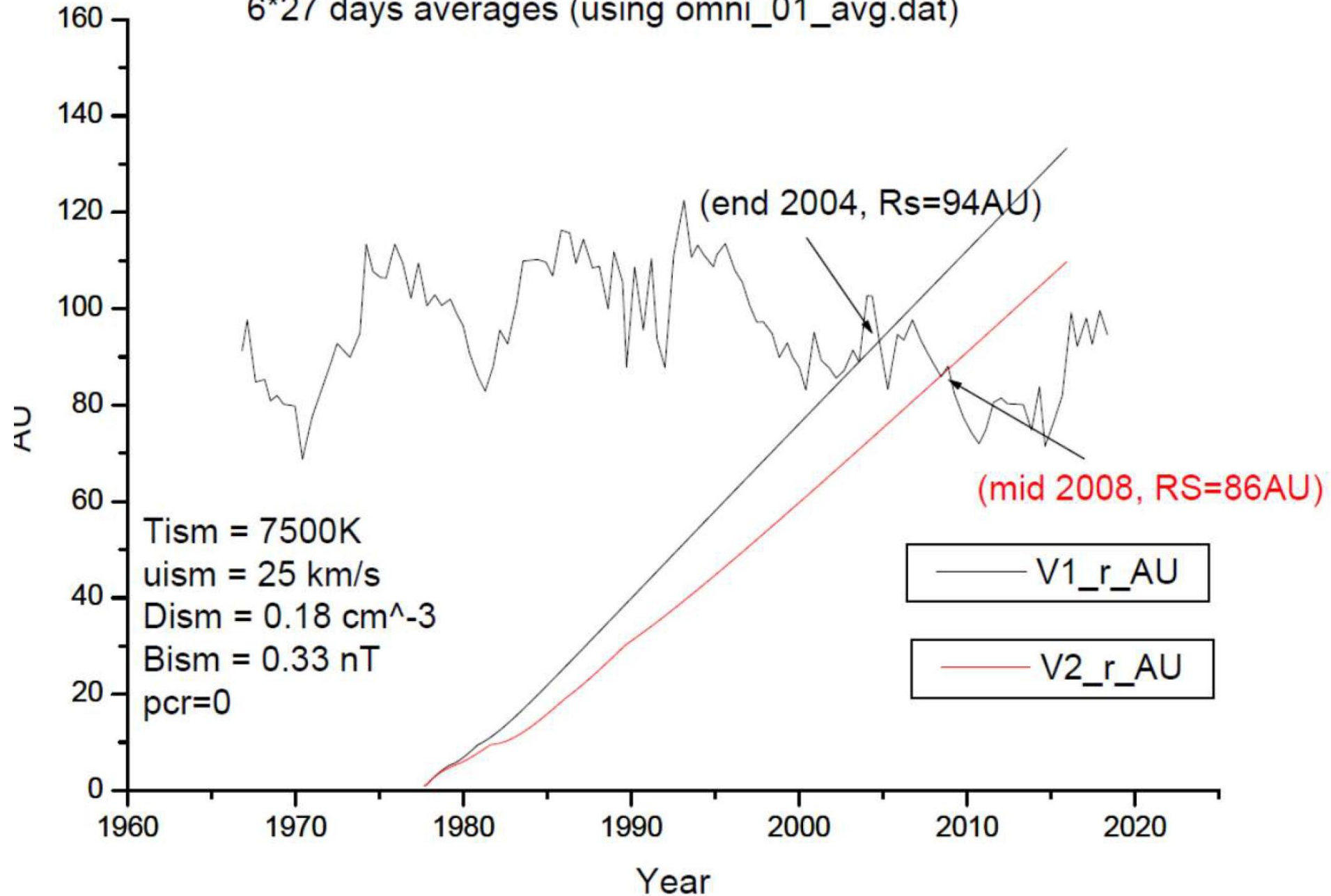
Both spacecraft are now exploring the shocked solar wind in the inner heliosheath.

They are heading toward the heliopause, the boundary that separates plasma of solar origin from the interstellar medium.



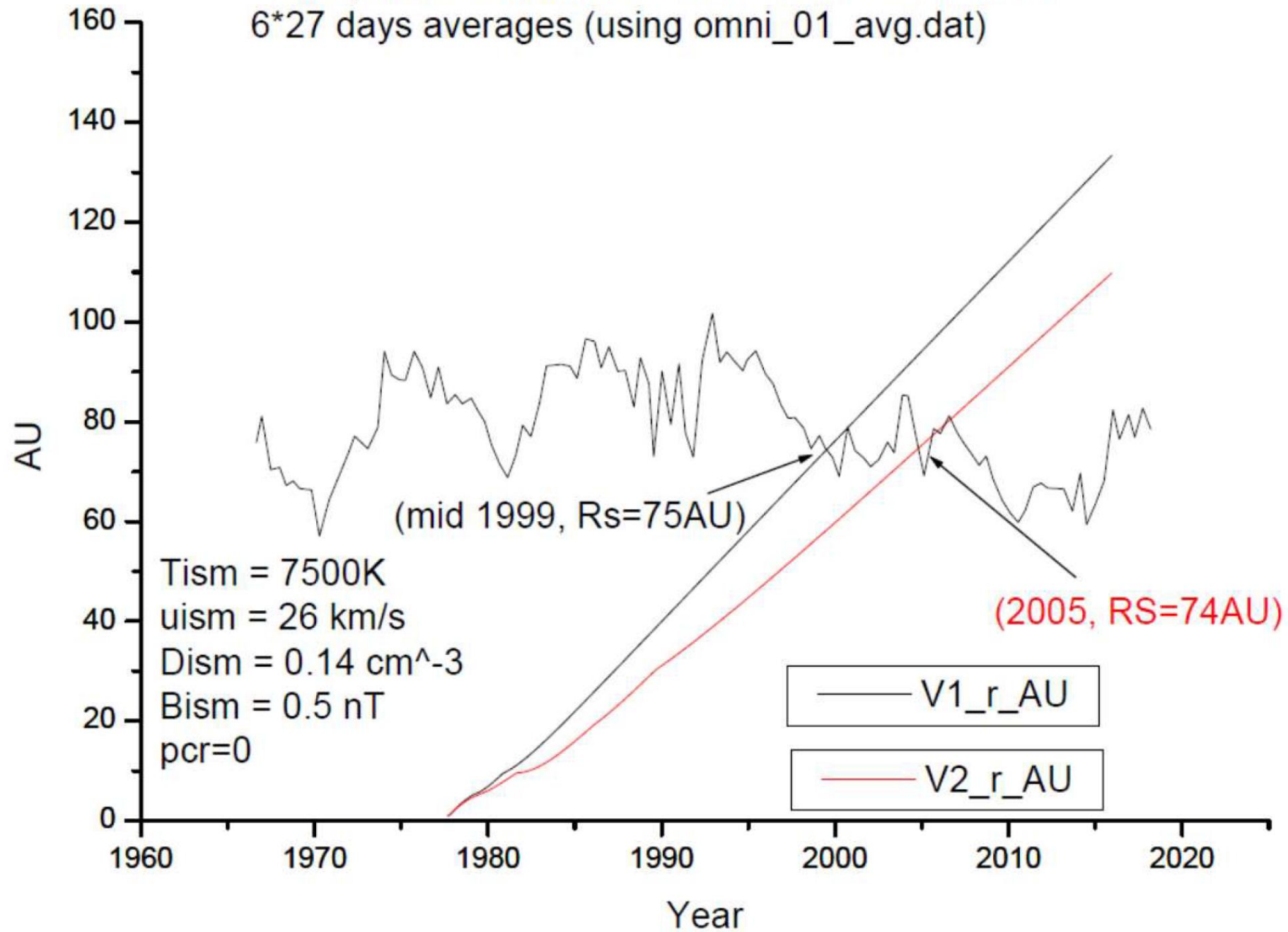
Heliospheric Termination Shock Radius Variations

6*27 days averages (using omni_01_avg.dat)

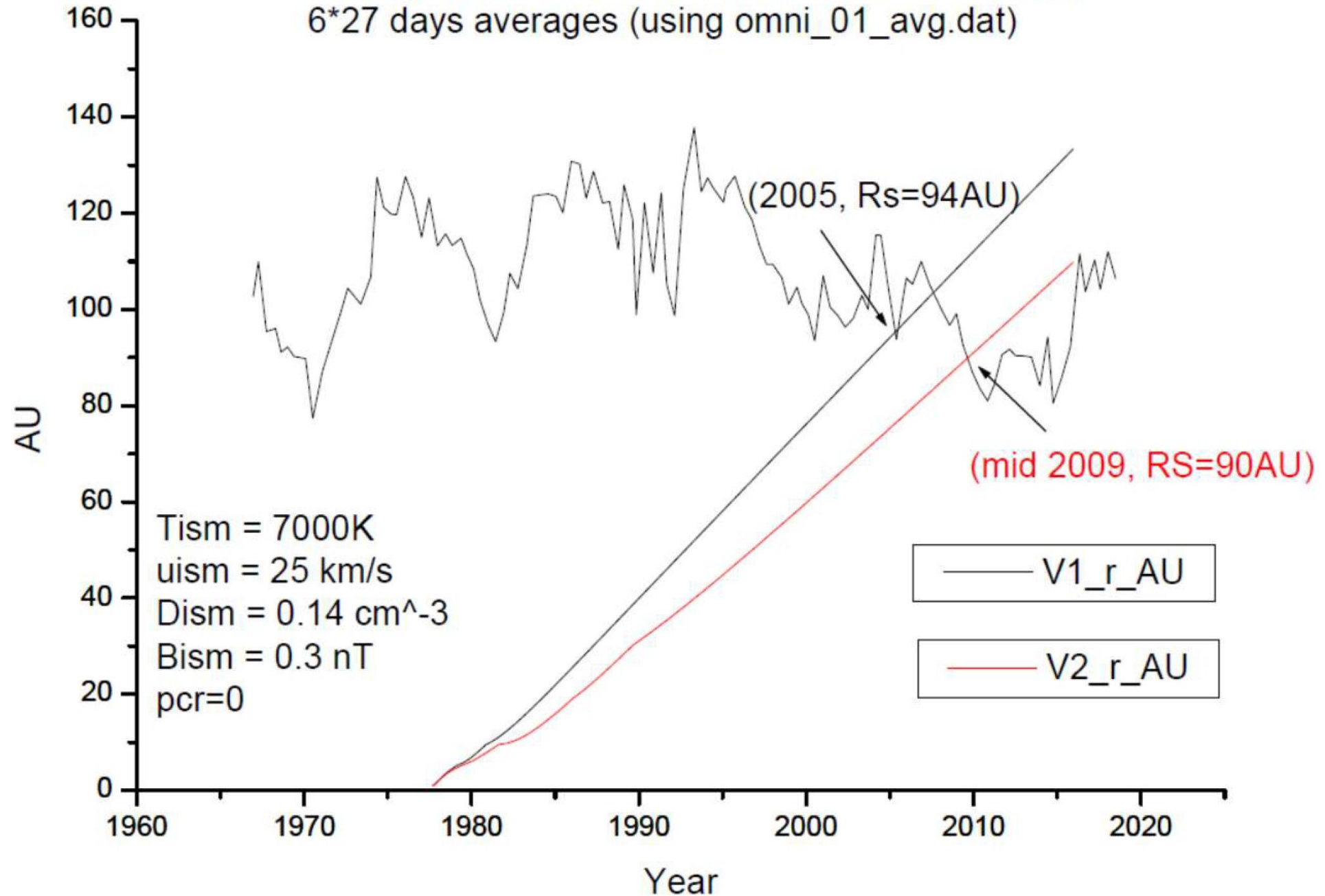


Heliospheric Termination Shock Radius Variations

6*27 days averages (using omni_01_avg.dat)

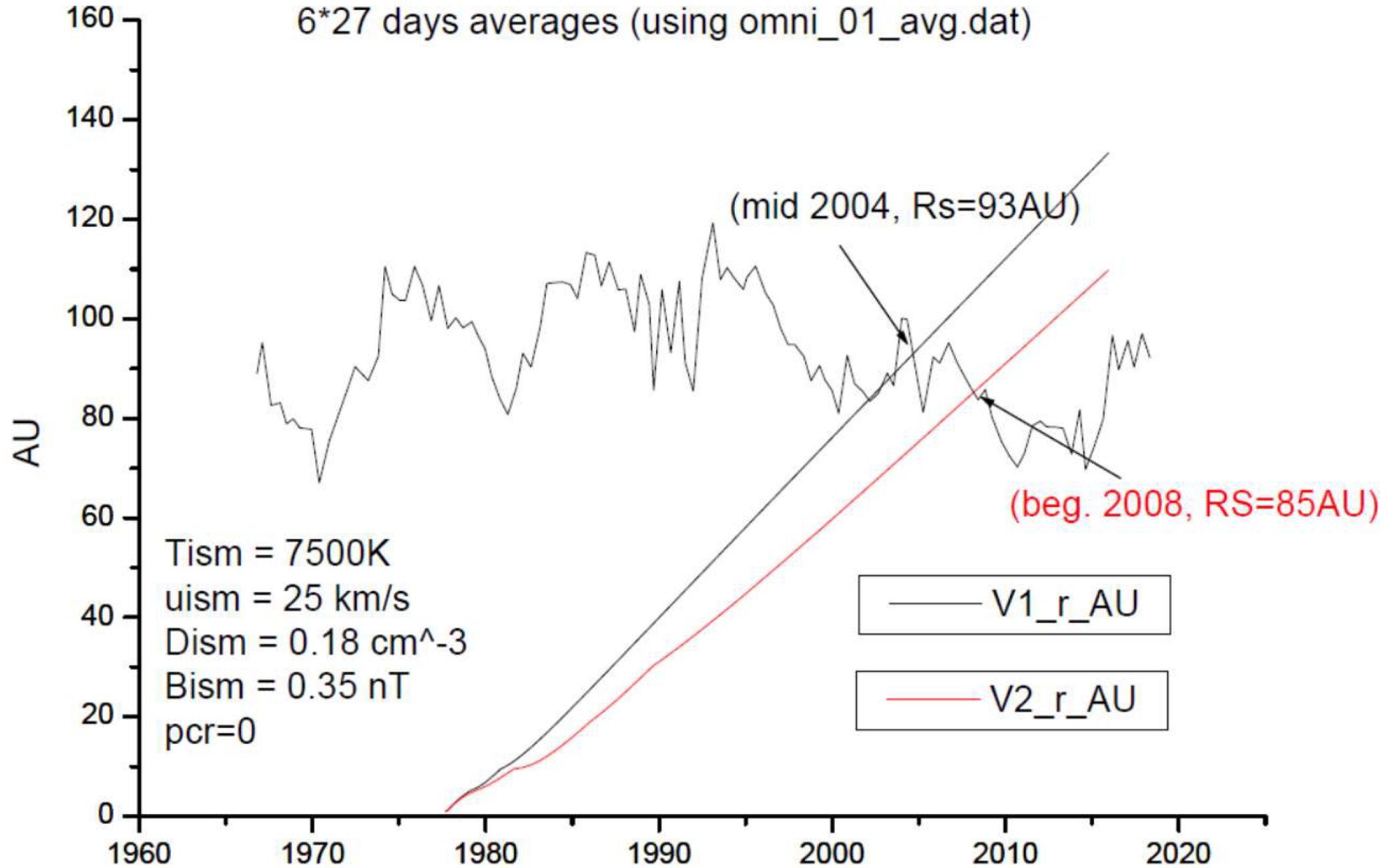


Heliospheric Termination Shock Radius Variations 6*27 days averages (using omni_01_avg.dat)



Heliospheric Termination Shock Radius Variations

6*27 days averages (using omni_01_avg.dat)

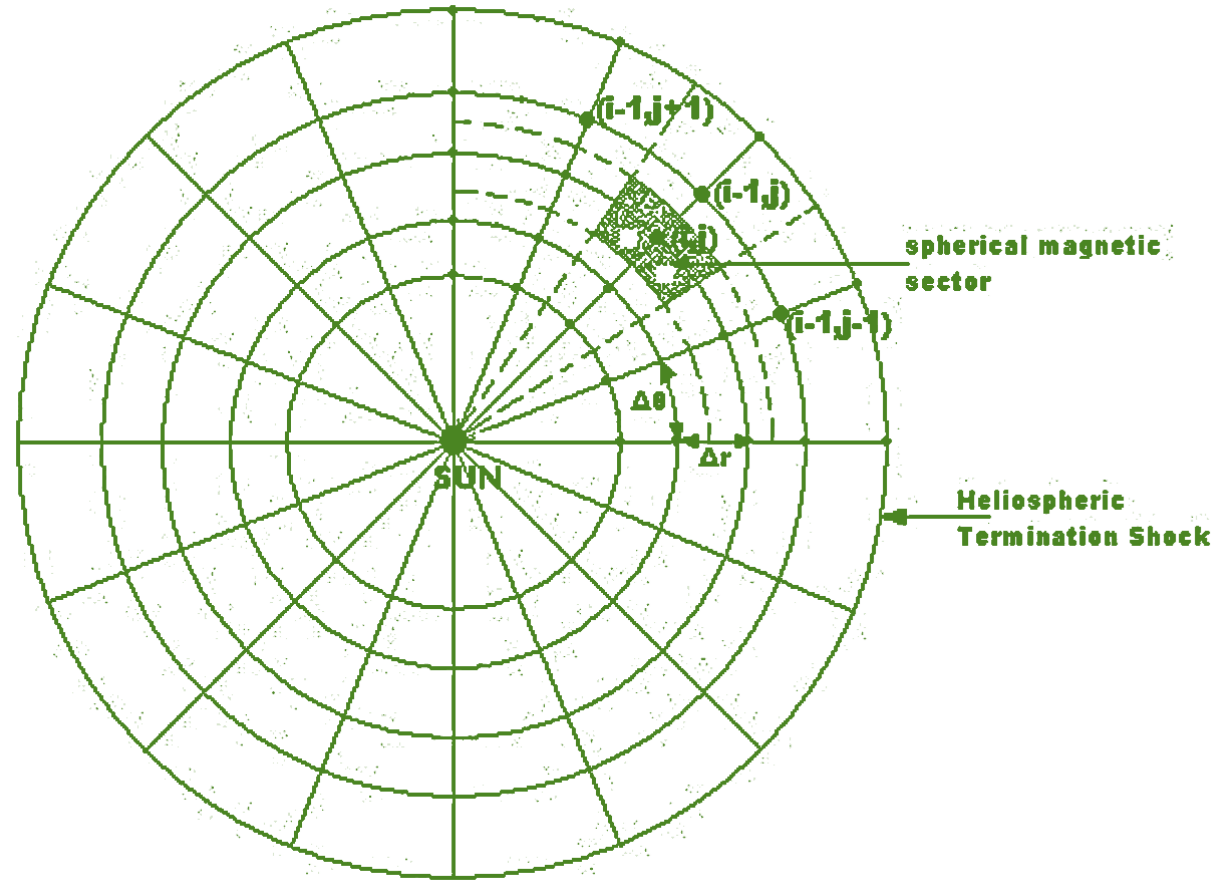


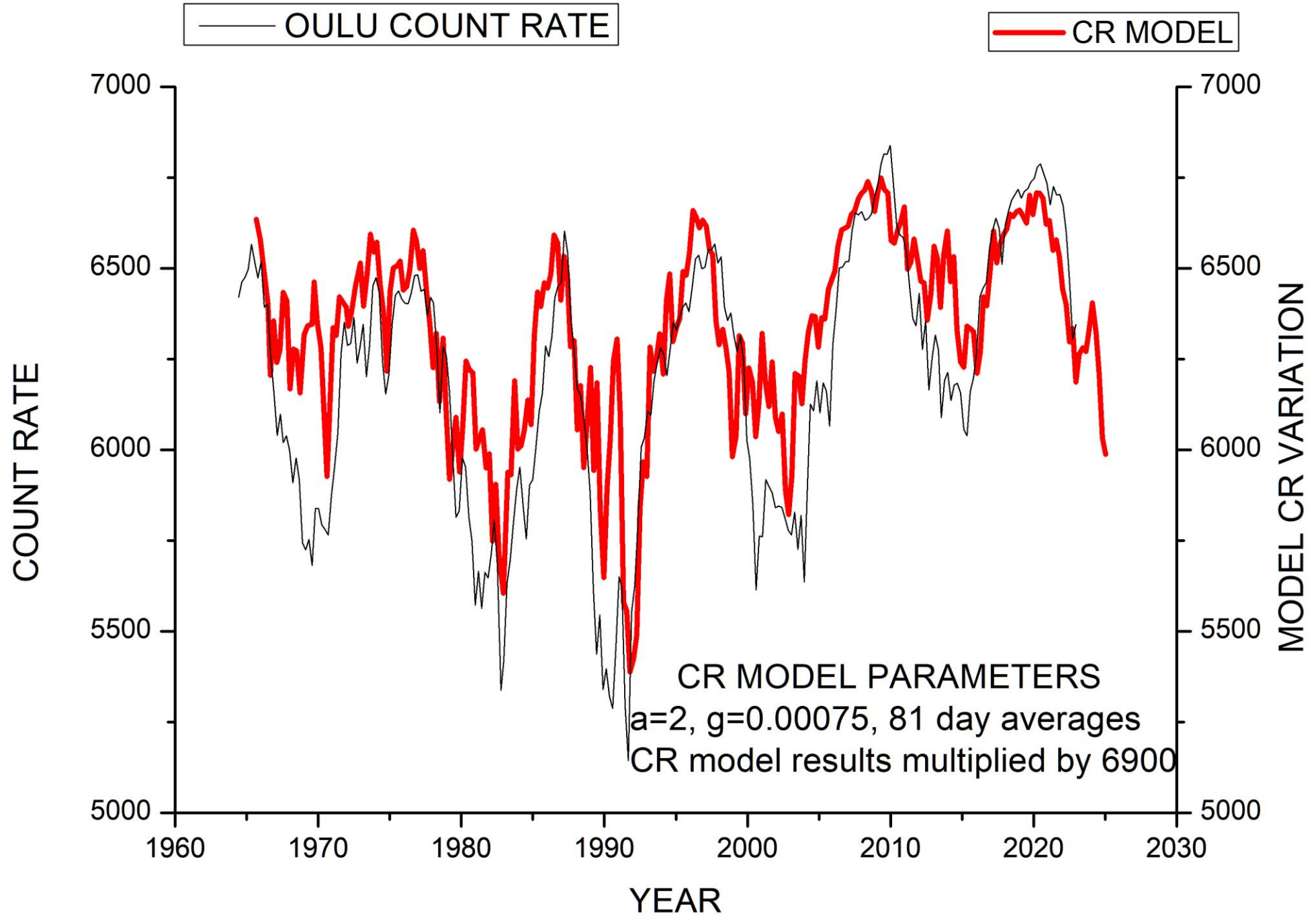
CR modulation

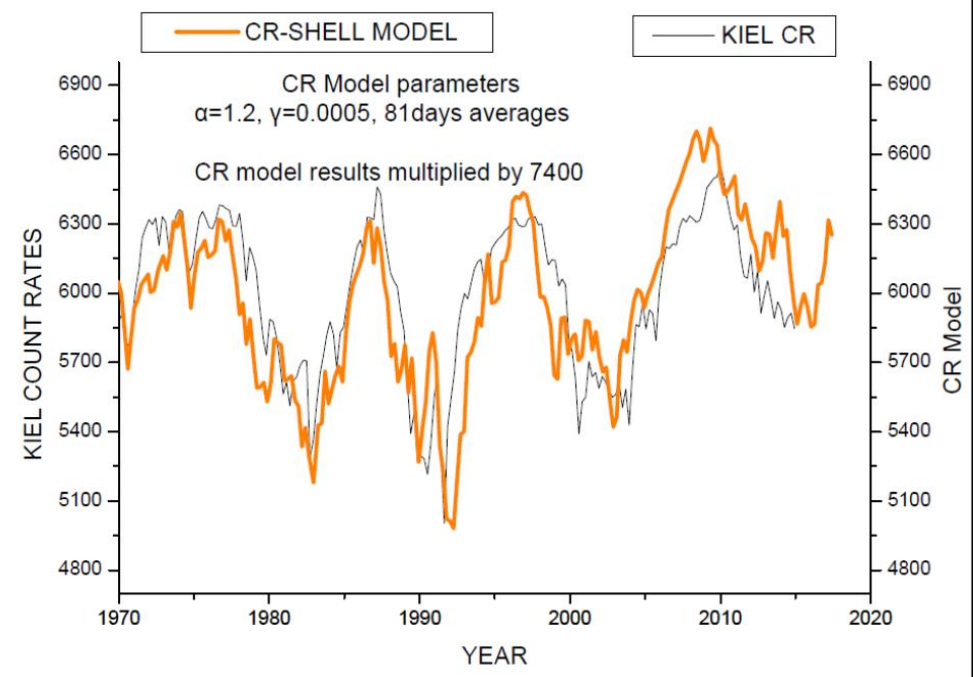
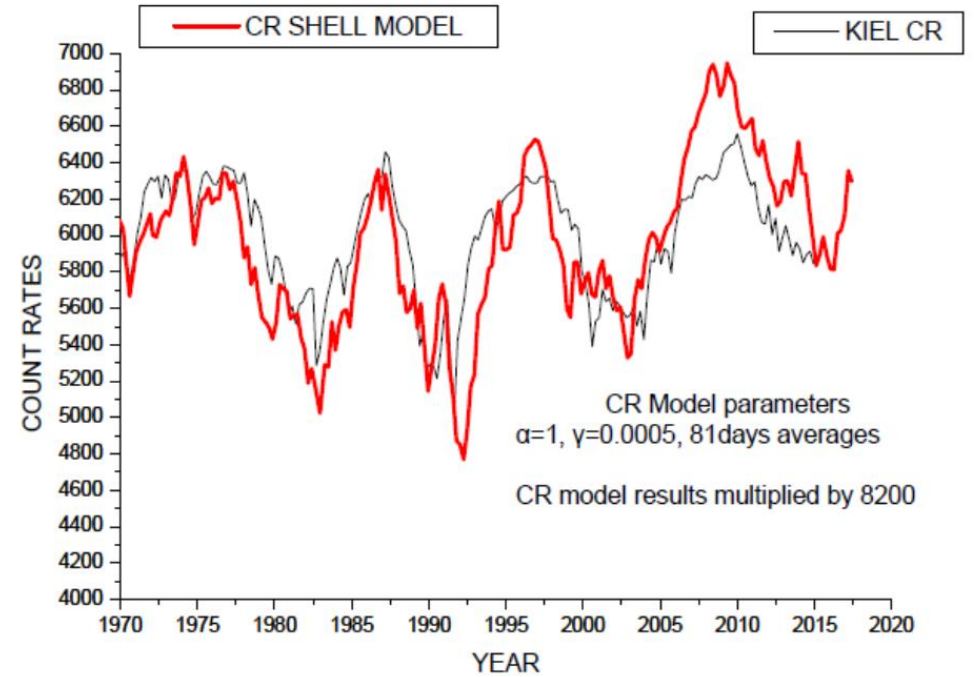
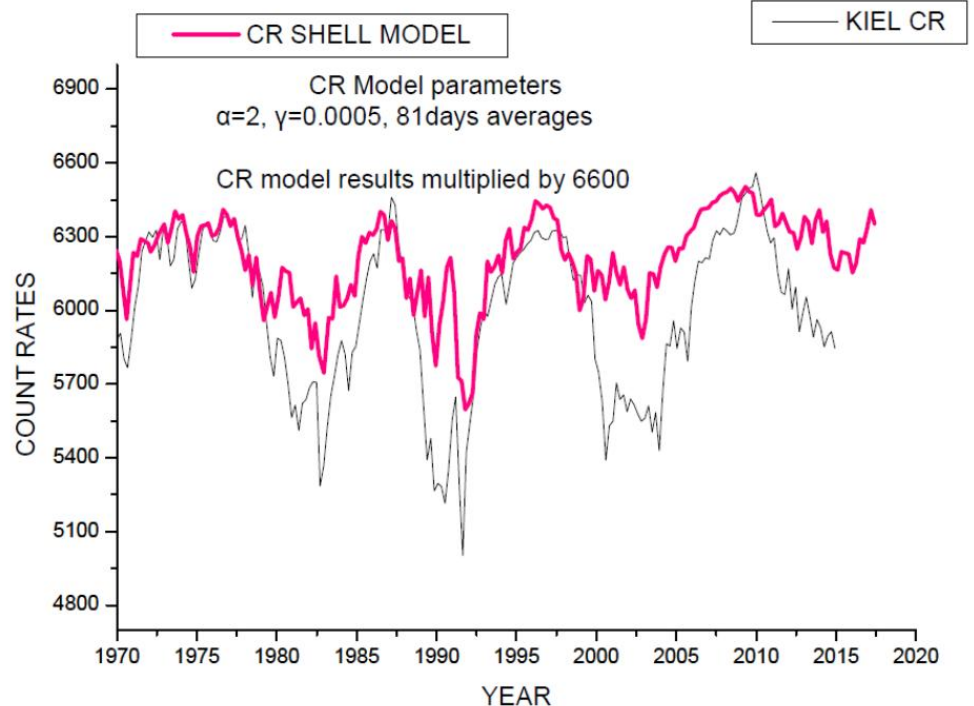
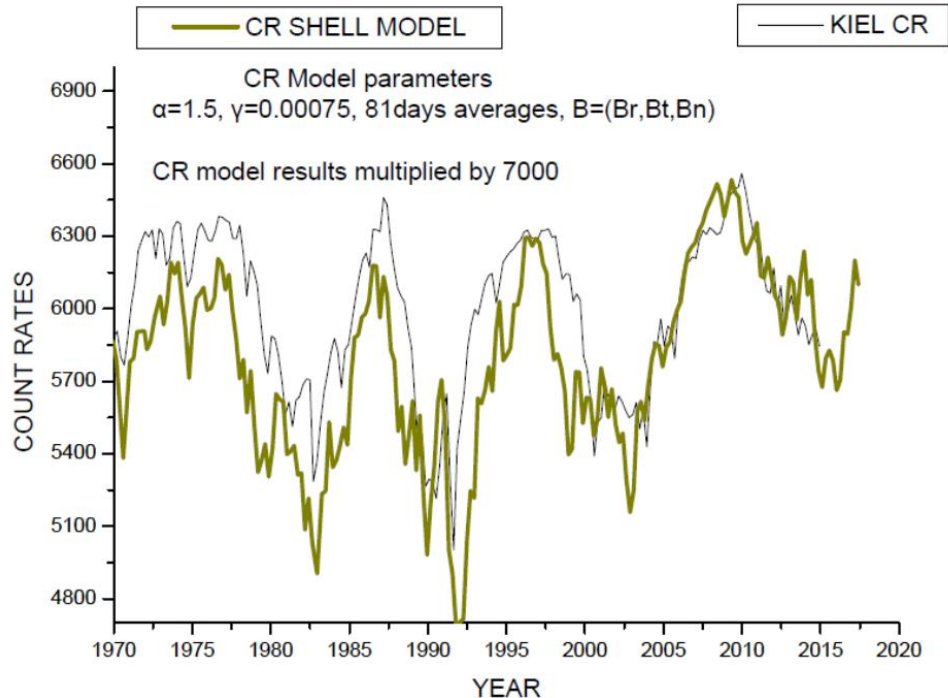
Using a simple diffusion-convection model (i.e. Parker 1965) assuming that the diffusion coefficient is proportional to $1/B^\alpha$.

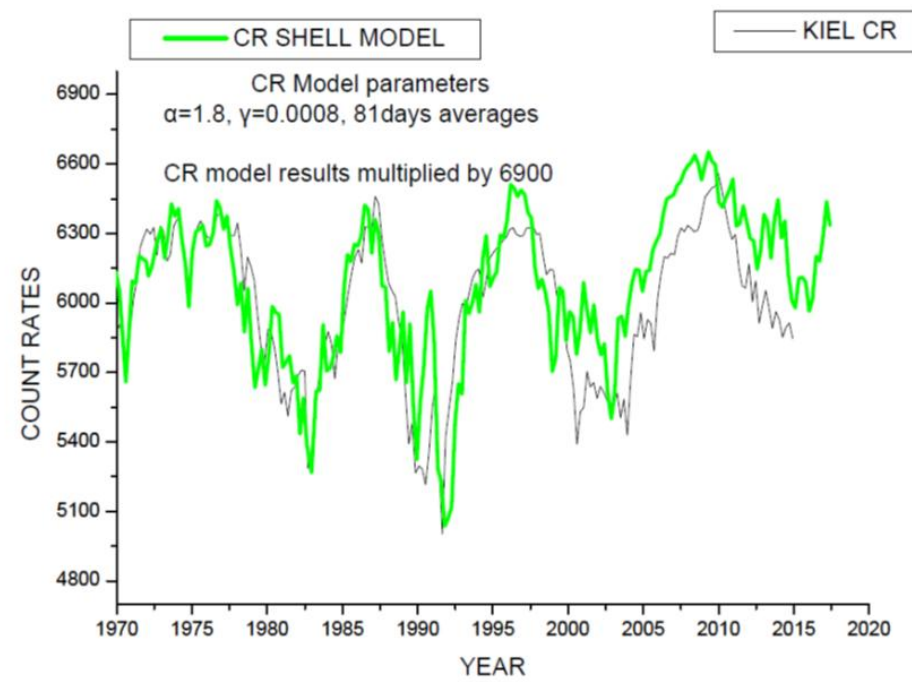
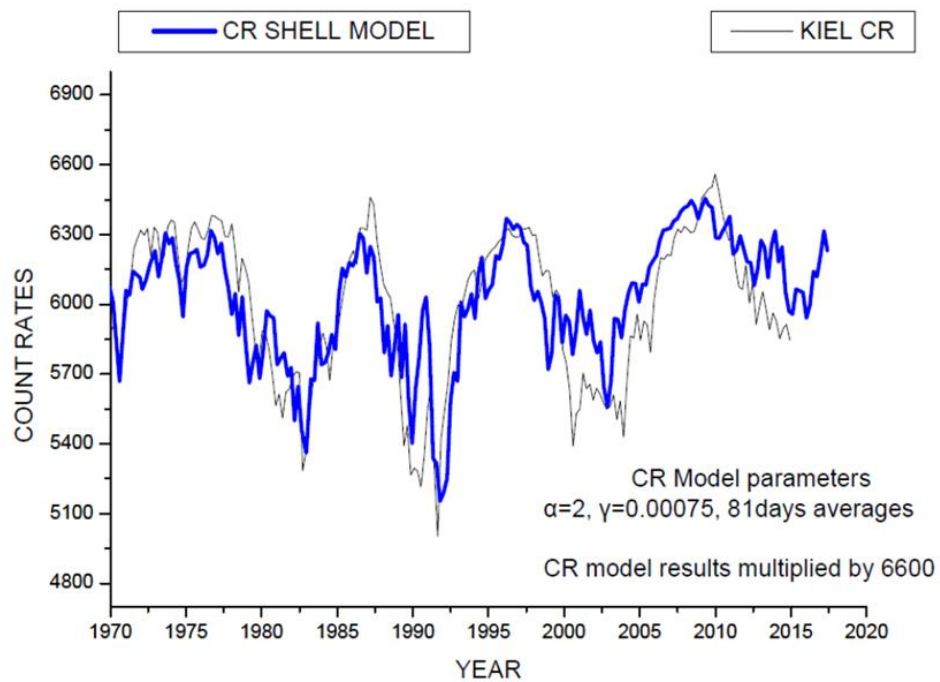
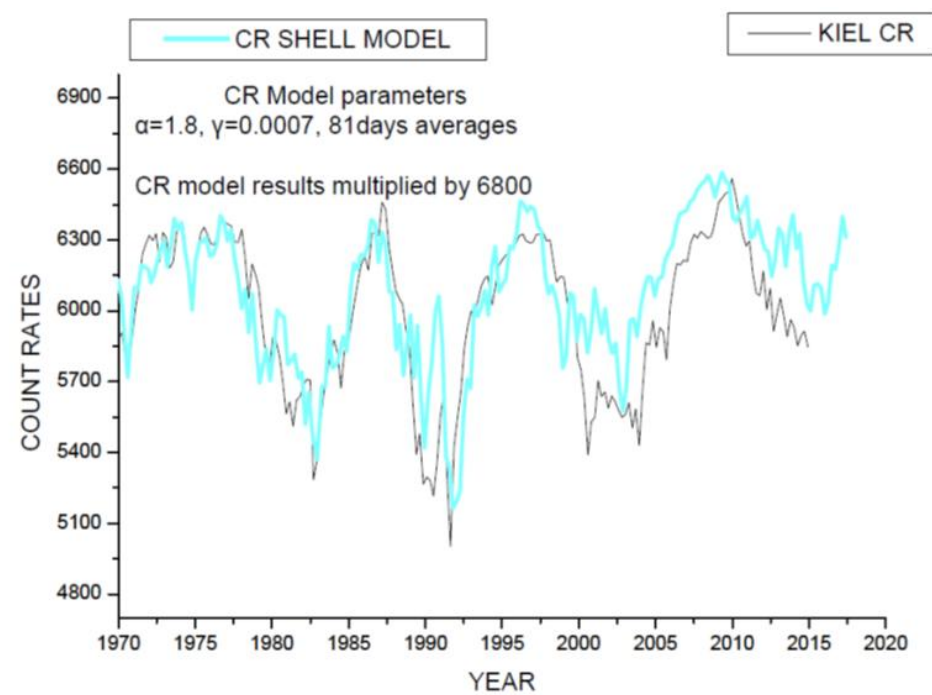
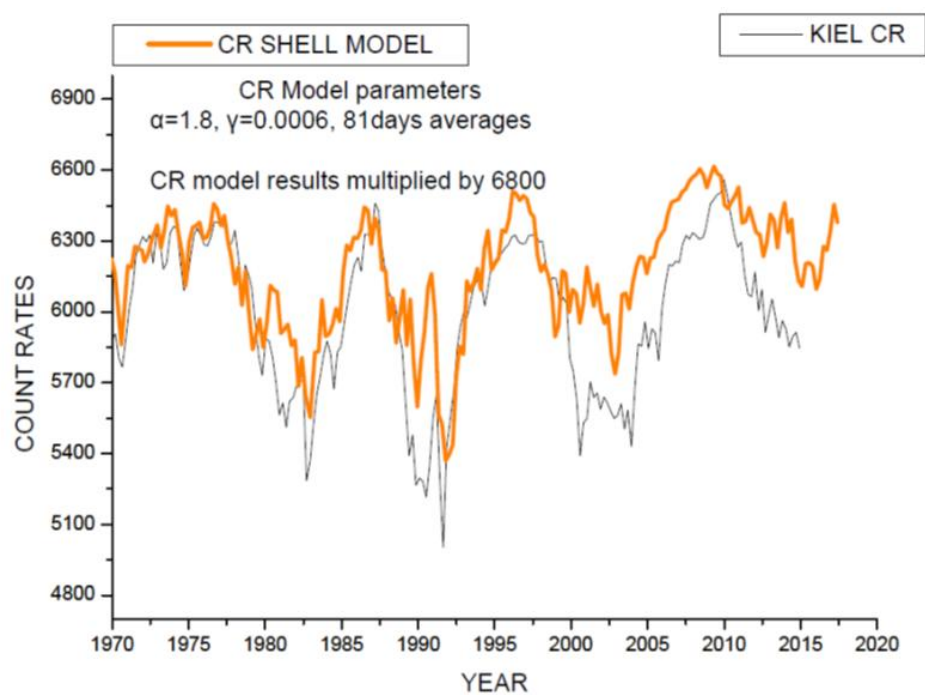
$$J = J_0 \exp(-\gamma u_{sw} B^\alpha)$$

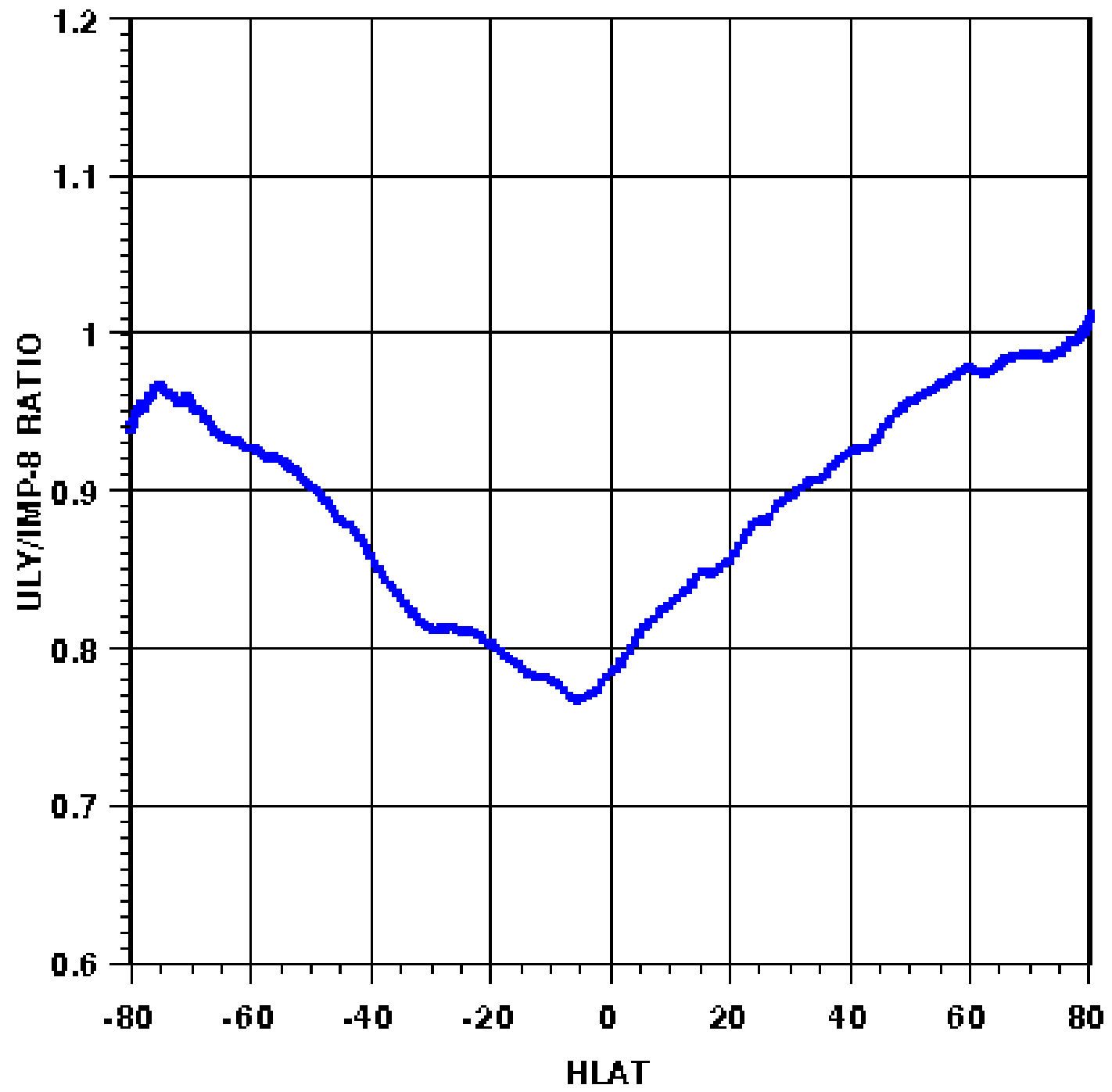
$$J(i, j) = \left(J(i-1, j) \exp(-\gamma_1 u_{sw} B_{(i-1, j)}^\alpha) \right. \\ \left. + J(i-1, j-1) \exp(\gamma_2 u_{sw} B_{(i-1, j-1)}^\alpha) \right. \\ \left. + J(i-1, j+1) \exp(-\gamma_3 u_{sw} B_{(i-1, j+1)}^\alpha) \right) / 3.0,$$

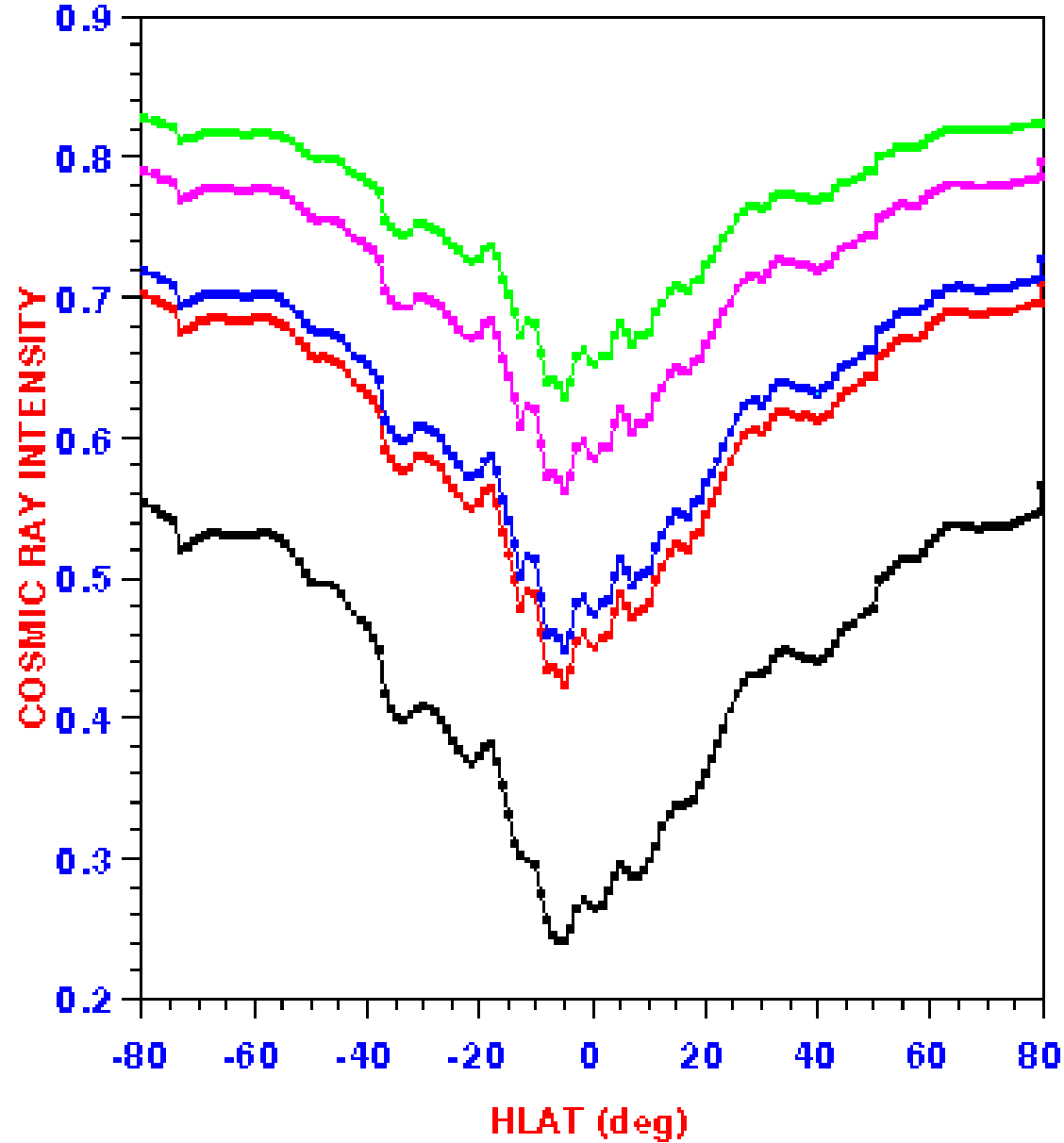










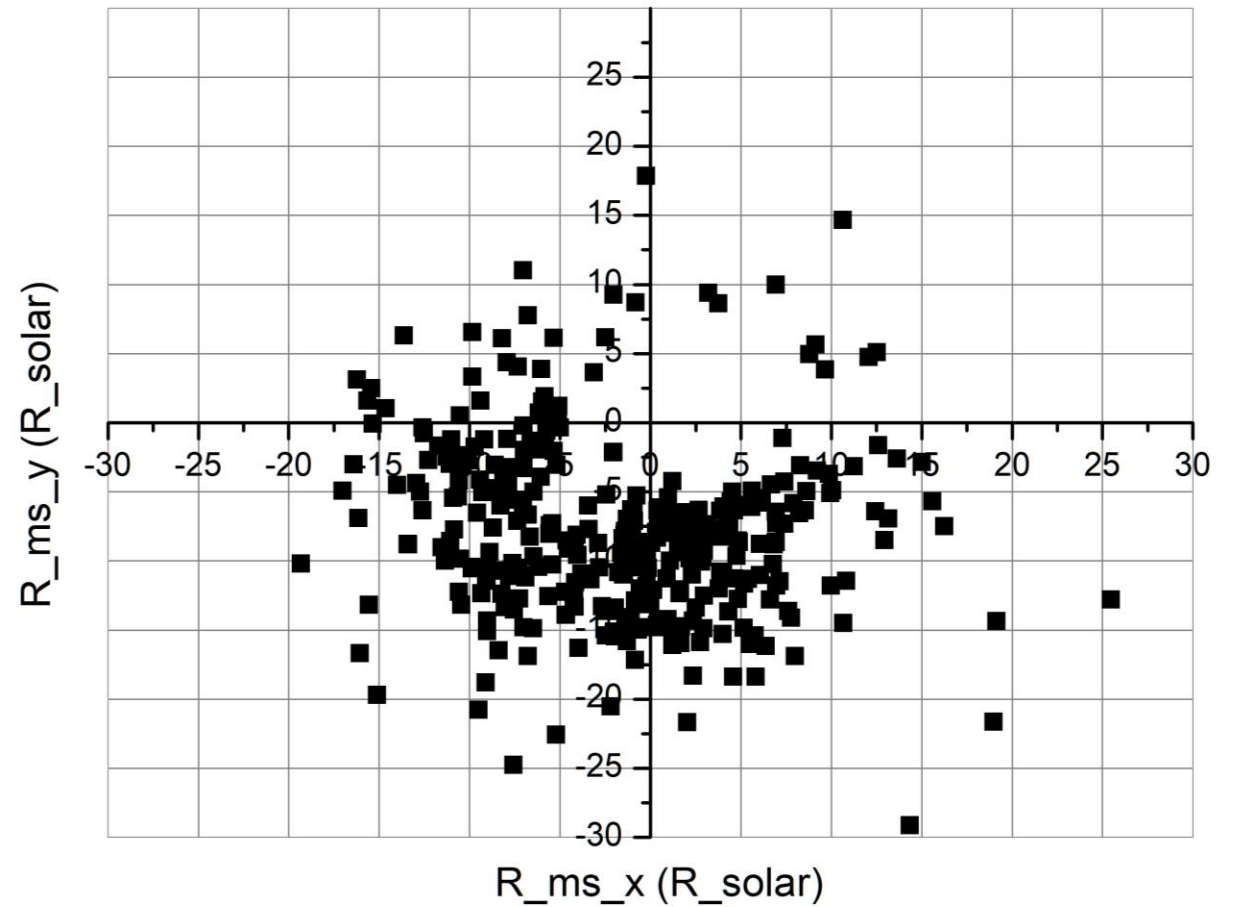


- $g1=0.07, g2=0.007$
- $g1=0.07, g2=0.01$
- $g1=0.04, g2=0.004$
- $g1=g2=0.05$
- $g1=0.05, g2=0.005$

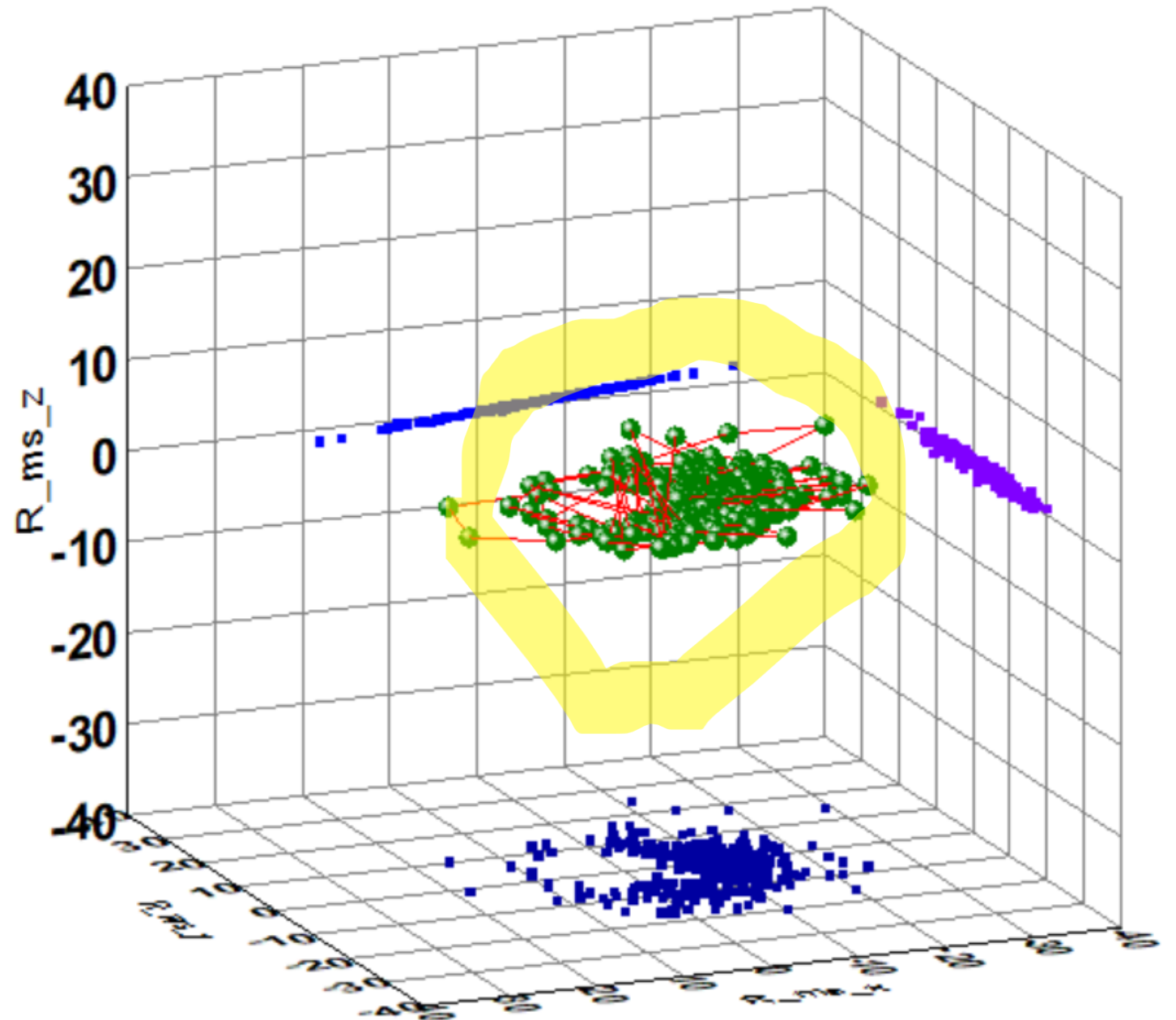
Magnetosonic surface

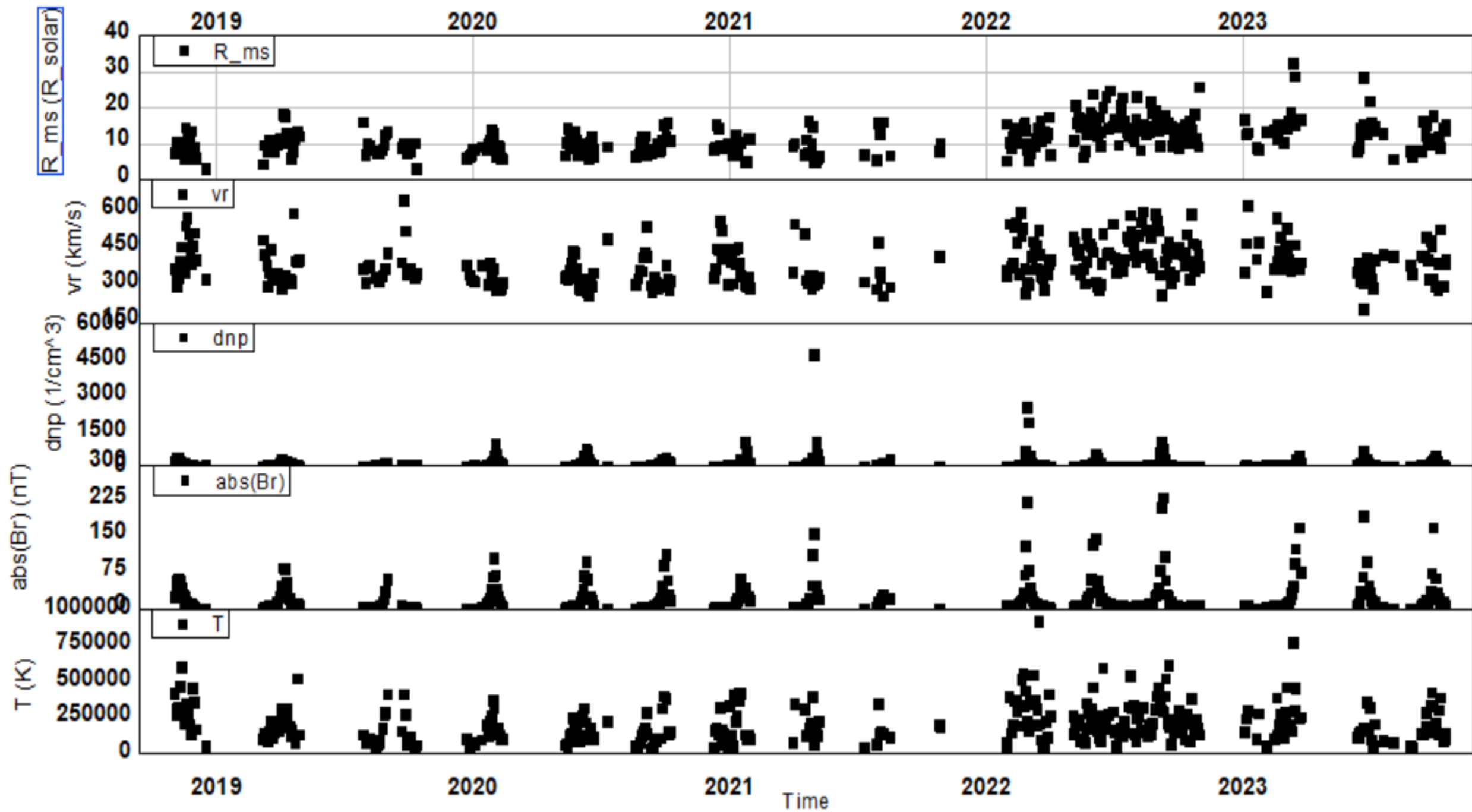
2 days average data from PSP hourly averages
(2018 - 2023)

■ Solar Wind Magnetosonic Radius (in Solar radii) - Equatorial plane



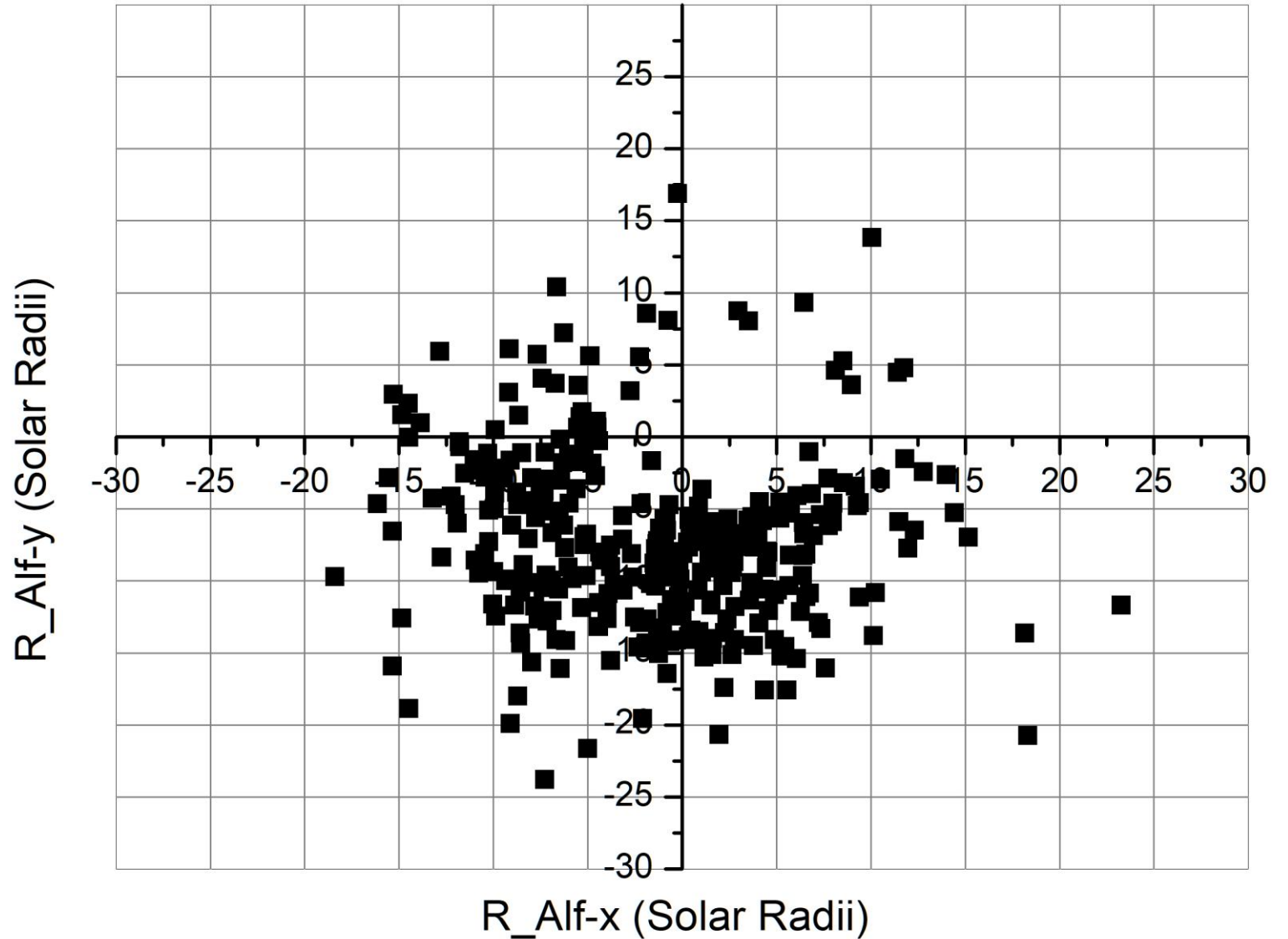
2 days average data from PSP hourly averages (2018 - 2023)





2 days average data from PSP hourly averages
(2018 - 2023)

■ Solar Wind Alfvén Radius (in Solar radii) - Equatorial plane

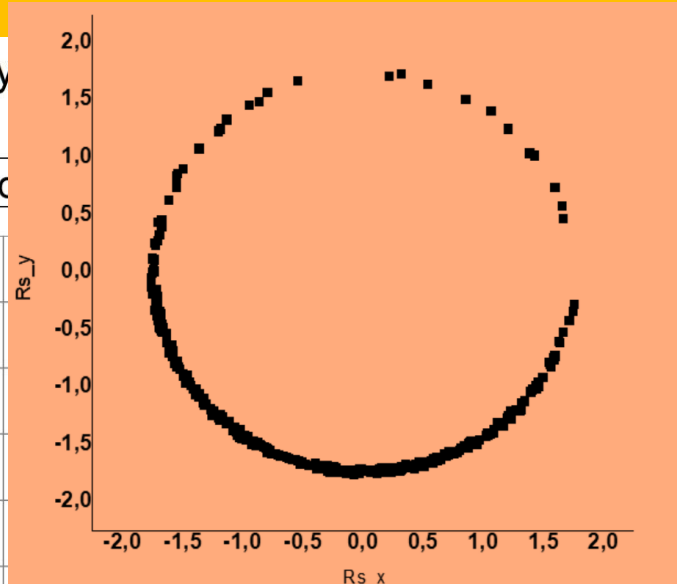
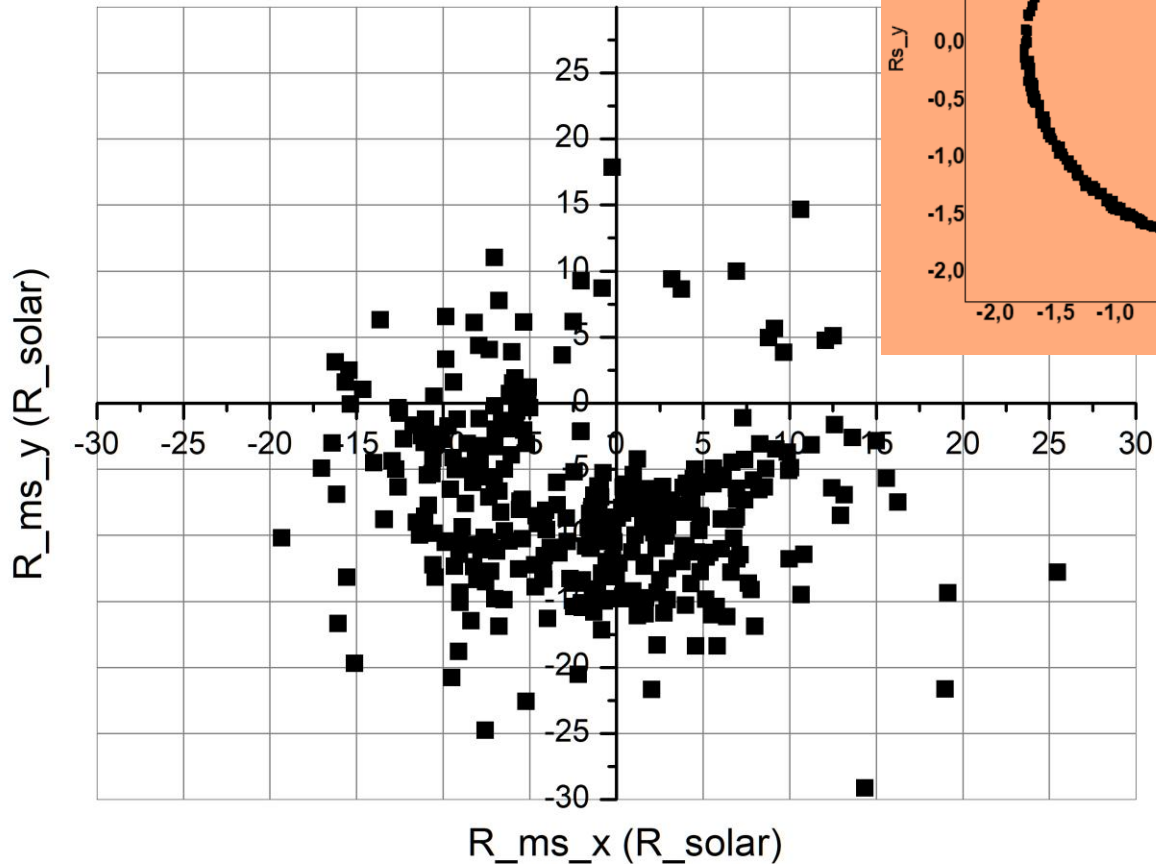


Alfvén
surface

As expected magnetosonic and Alfvén surfaces coincide

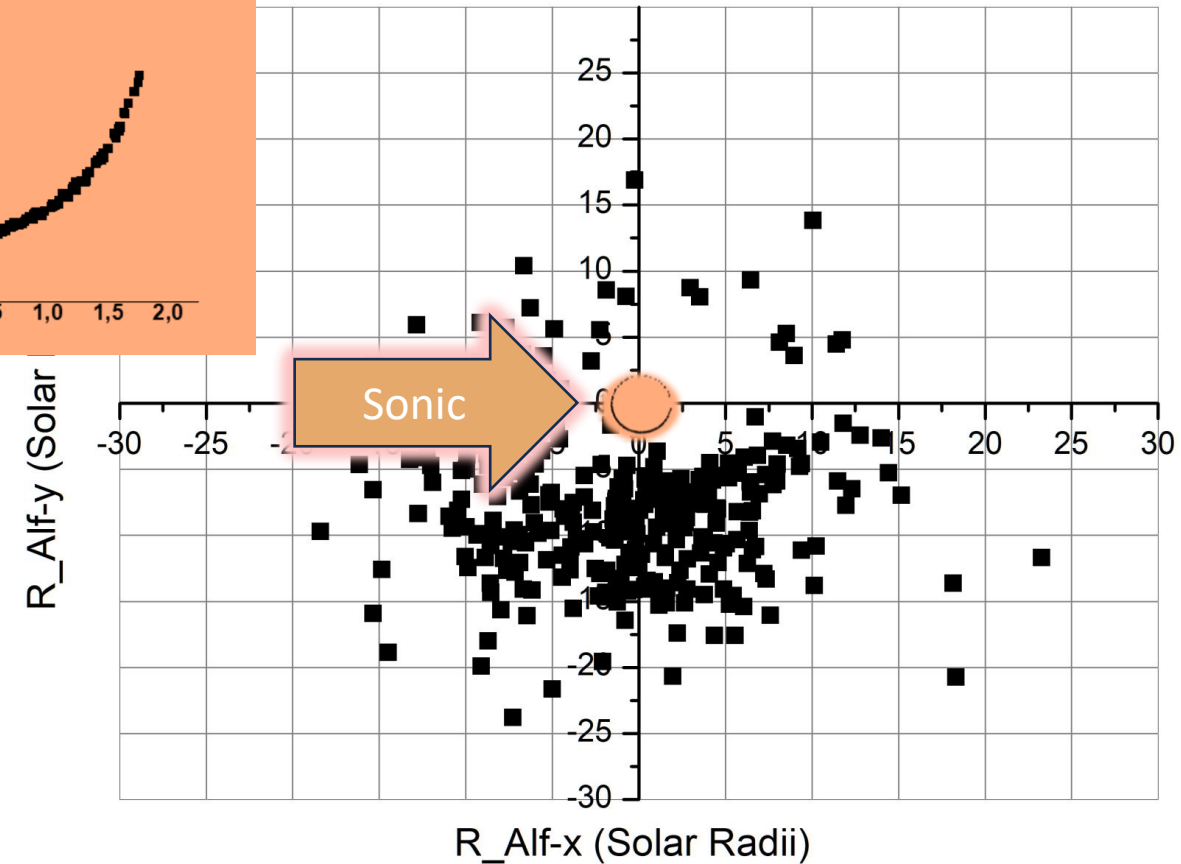
2 days average data from PSP hourly
(2018 - 2023)

■ Solar Wind Magnetosonic Radius (in Solar radii)



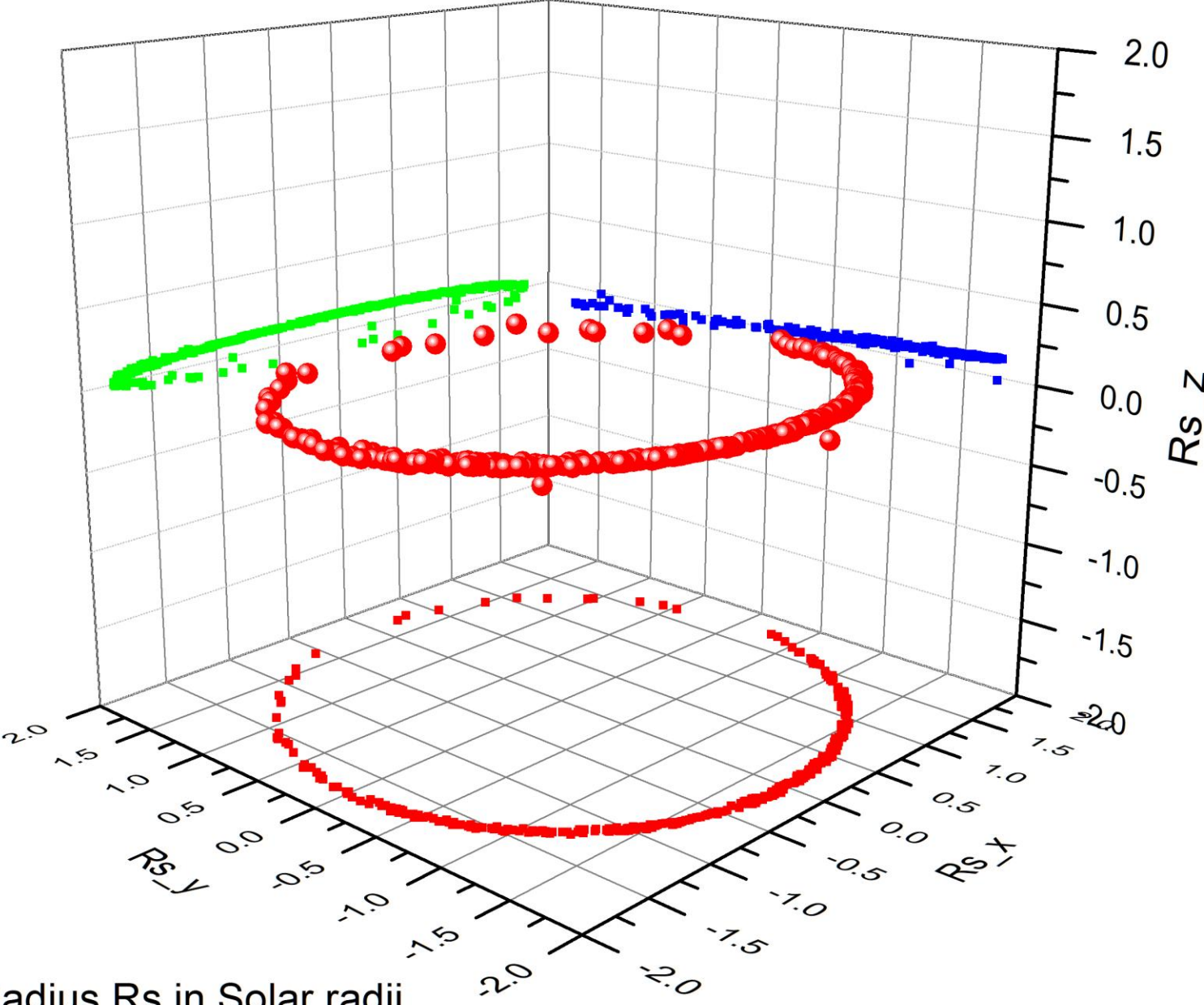
2 days average data from PSP hourly averages
(2018 - 2023)

■ Solar Wind Alfvén Radius (in Solar radii) - Equatorial plane



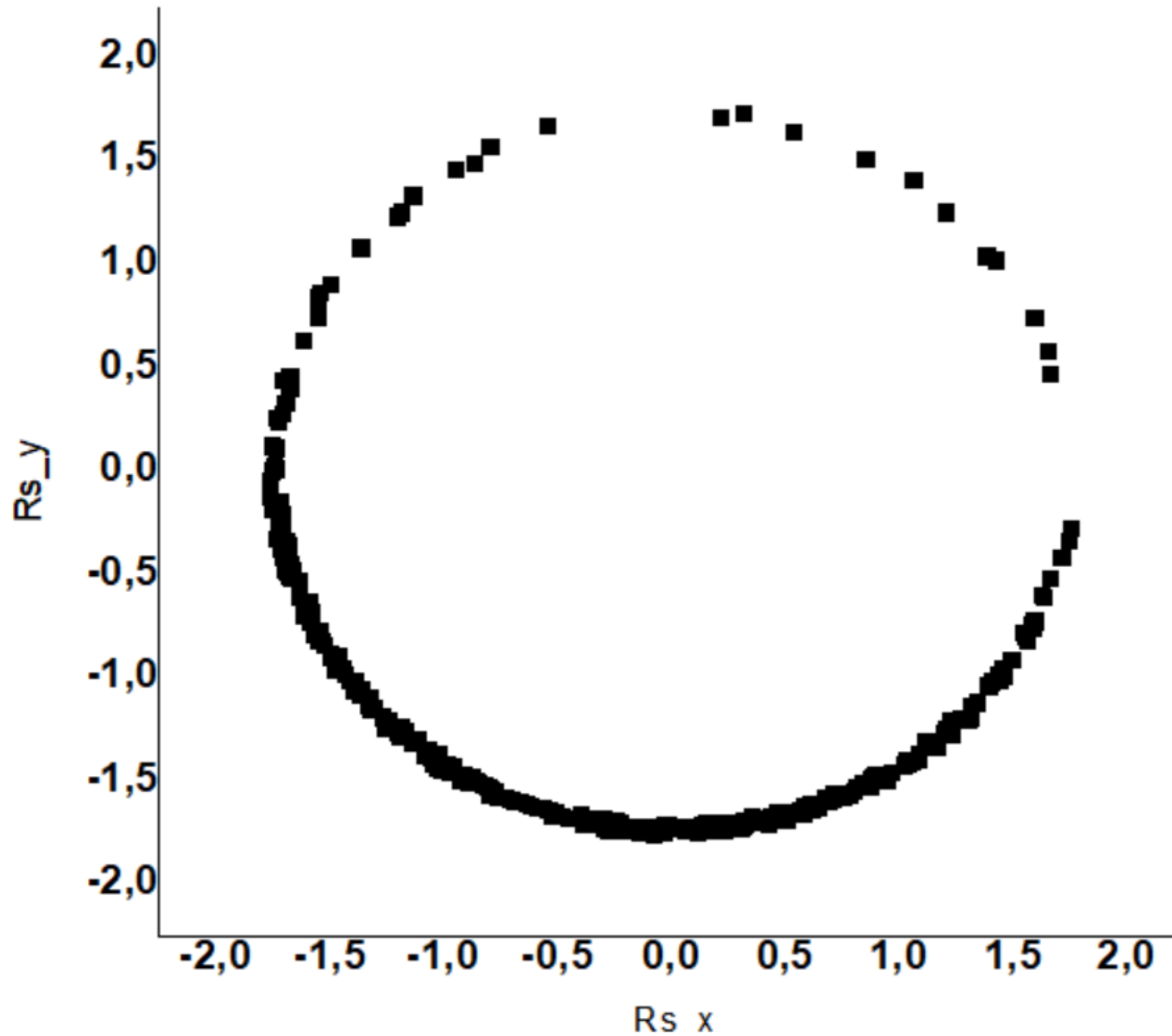
2 days average data from PSP hourly averages (2018-2023)

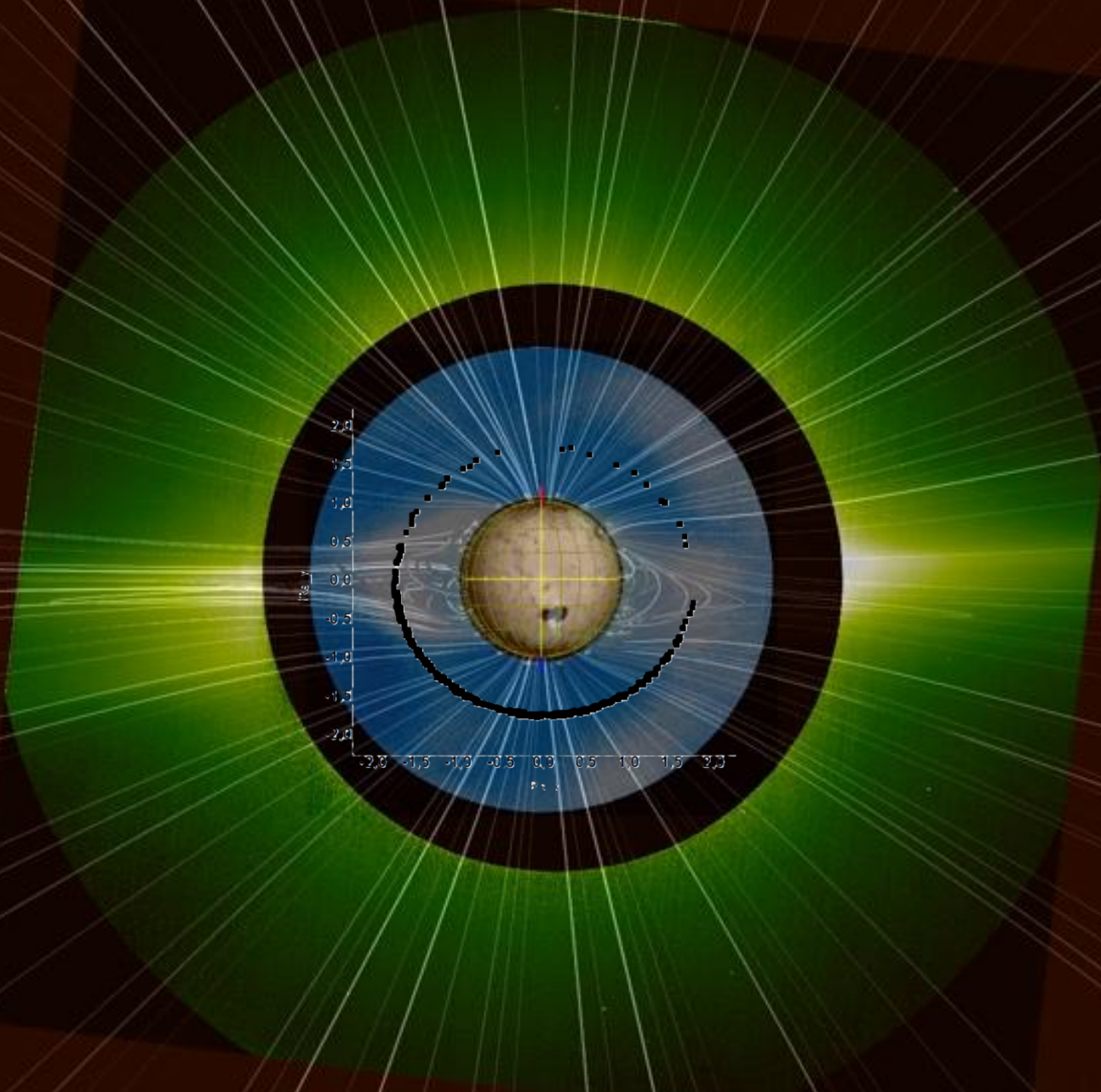
Sonic surface



Sonic Radius R_s in Solar radii

Sonic surface



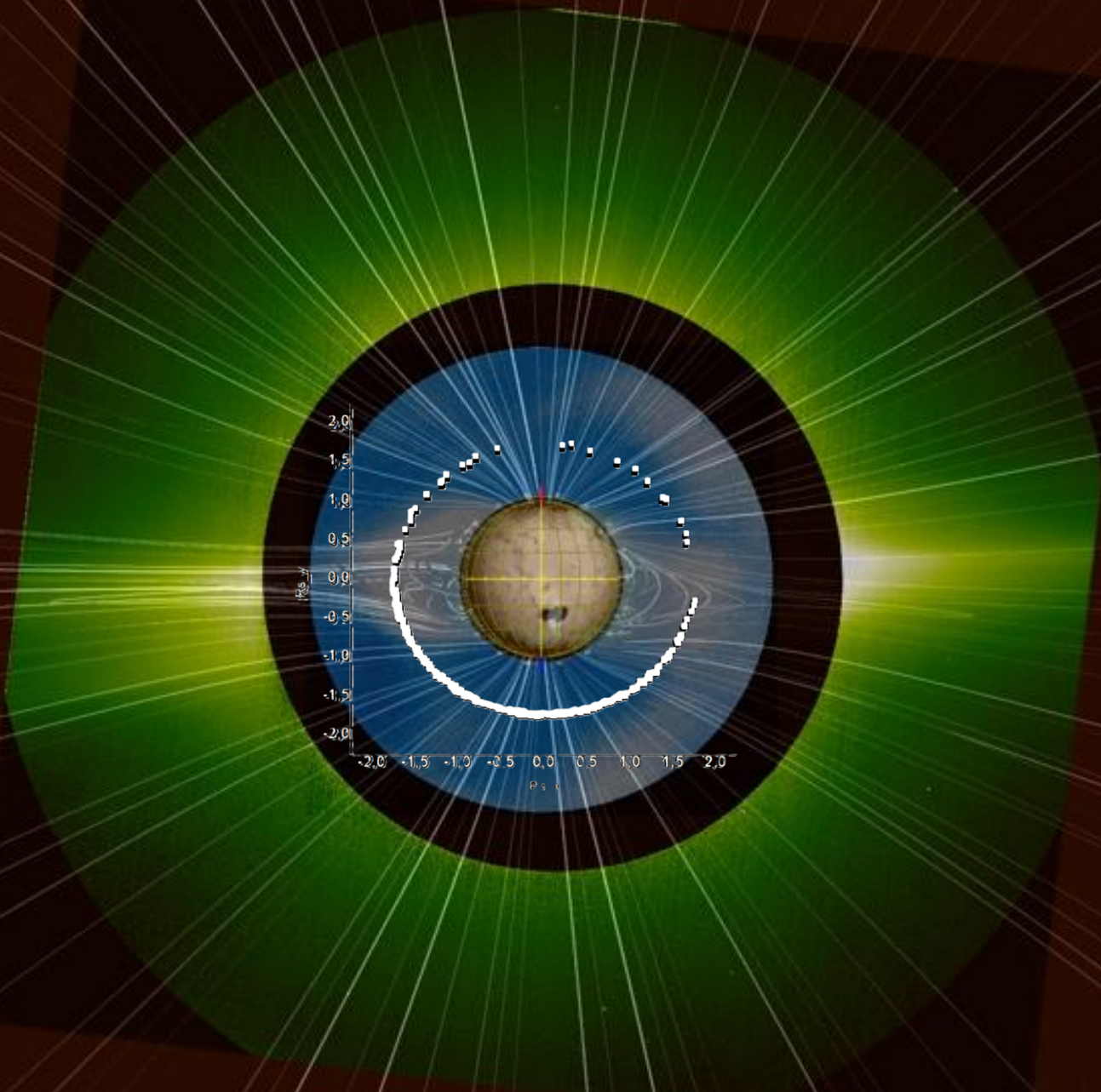


CREDIT

data NSSDCA, PSP OMNI

Solar Orbiter/Metis Team/
ESA & NASA; Mauna Loa
Solar

Observatory/HAO/NaCAR
/NSF; Predictive Science
Inc./NASA/NSF/AFOSR;
NASA/SDO/AIA

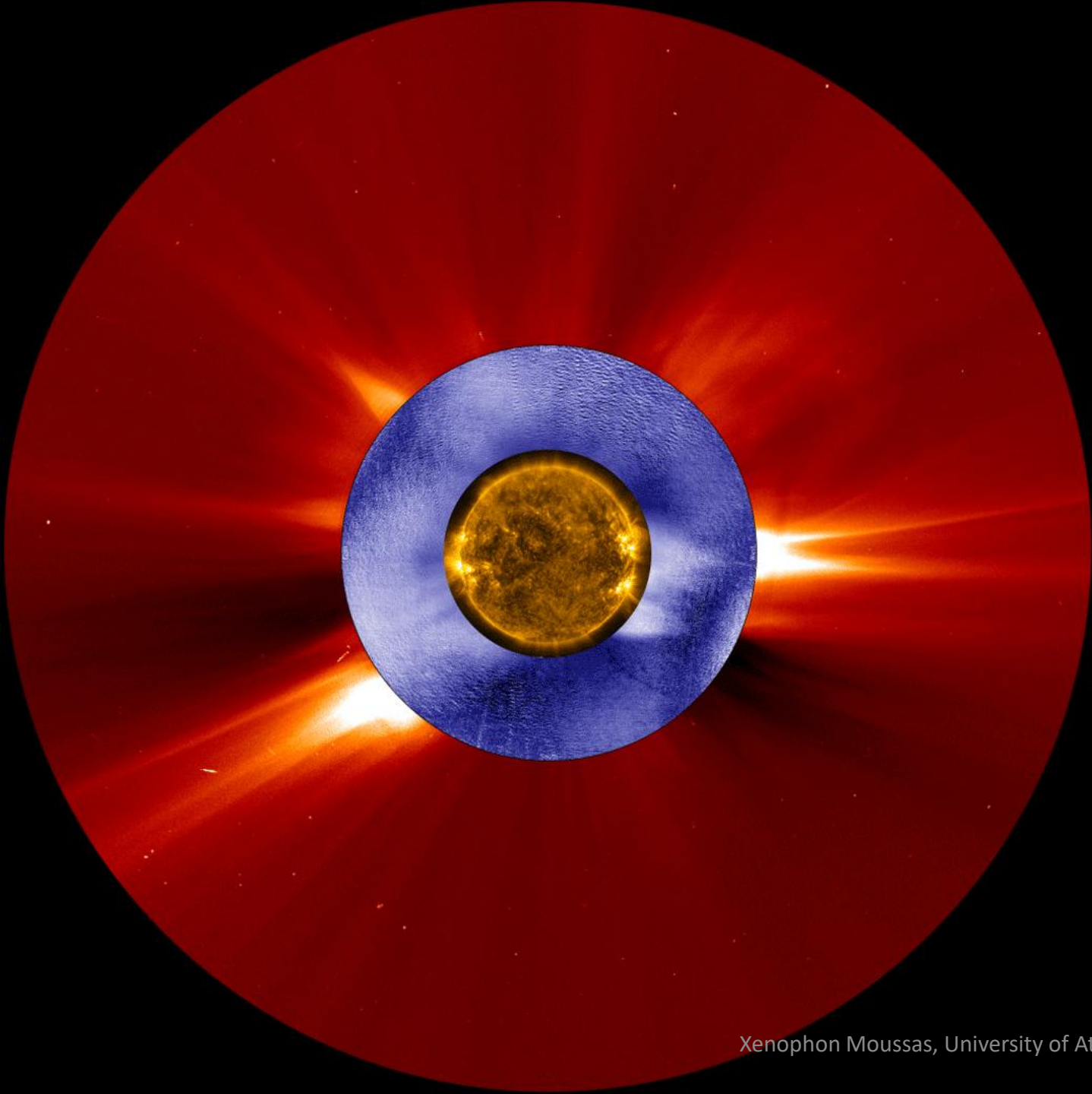


CREDIT

data NSSDCA, PSP OMNI

Solar Orbiter/Metis Team/
ESA & NASA; Mauna Loa
Solar

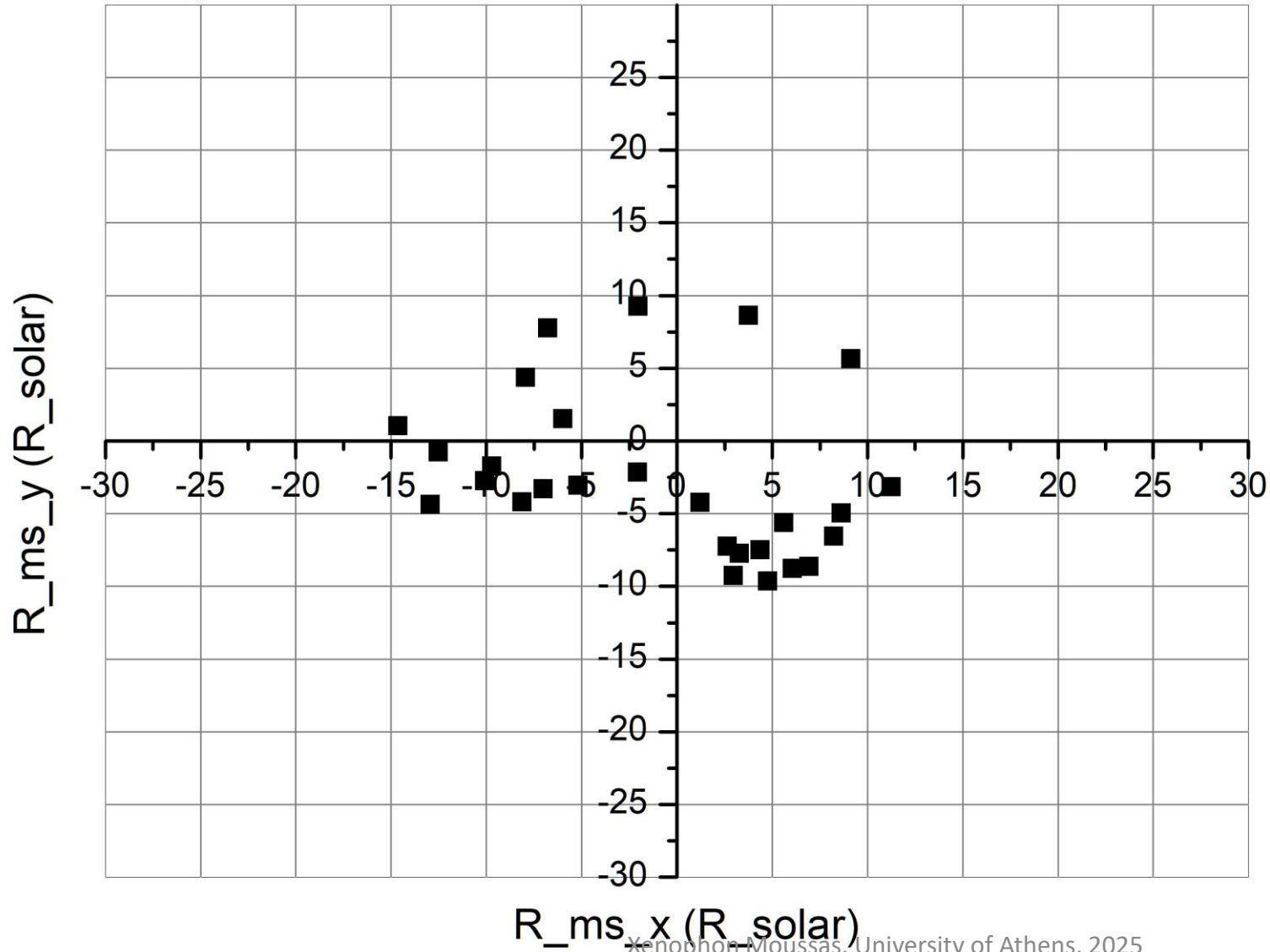
Observatory/HAO/NaCAR
/NSF; Predictive Science
Inc./NASA/NSF/AFOSR;
NASA/SDO/AIA



credit: NASA/ESA/SOHO/SDO/Joy Ng
and MLSO/K-Cor)

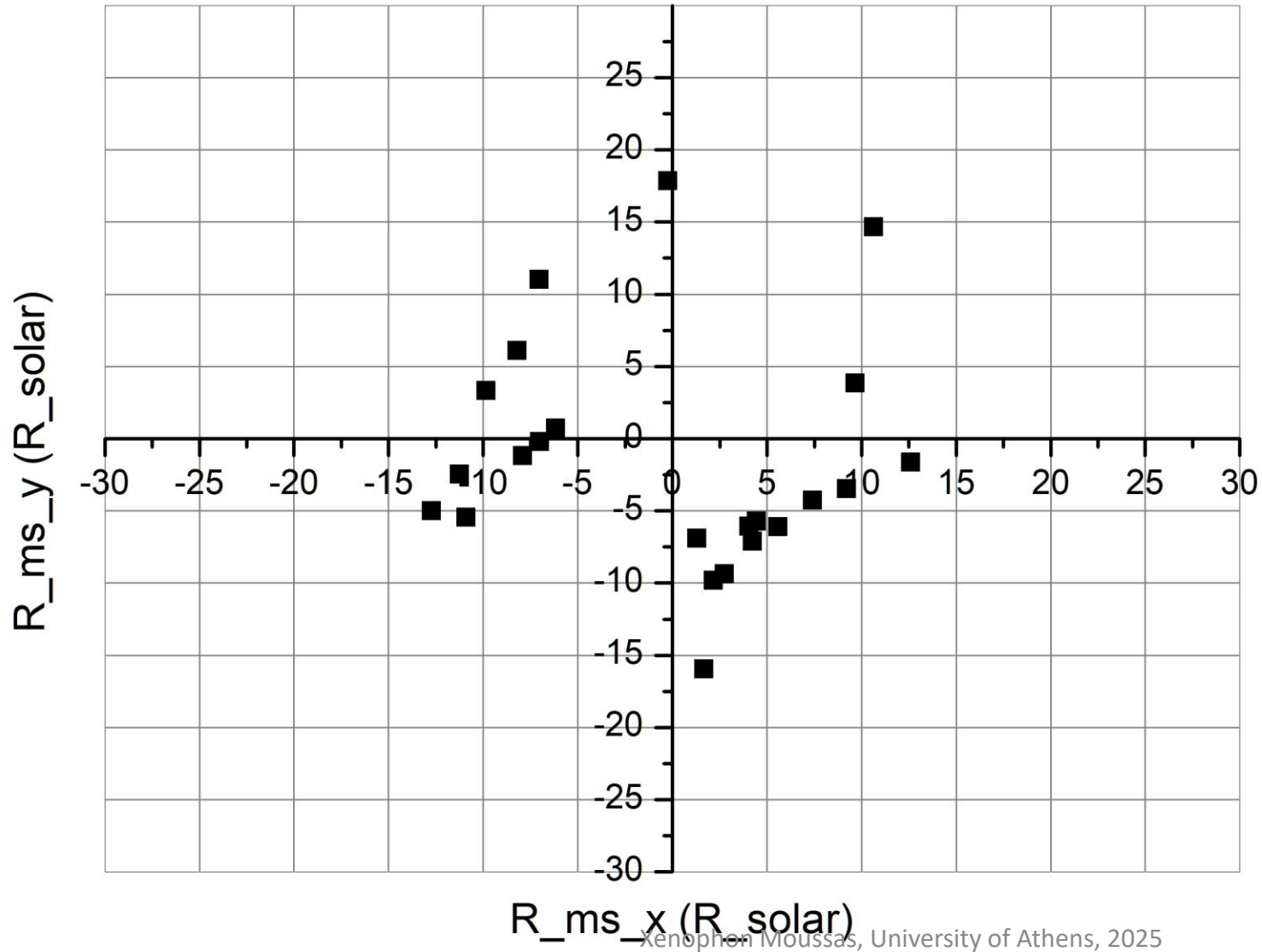
2 days average data from PSP hourly averages
(2018 D:307 - 2019 D:88, 1 rotation around Sun)

■ Solar Wind Magnetosonic Radius (in Solar radii) - Equatorial plane



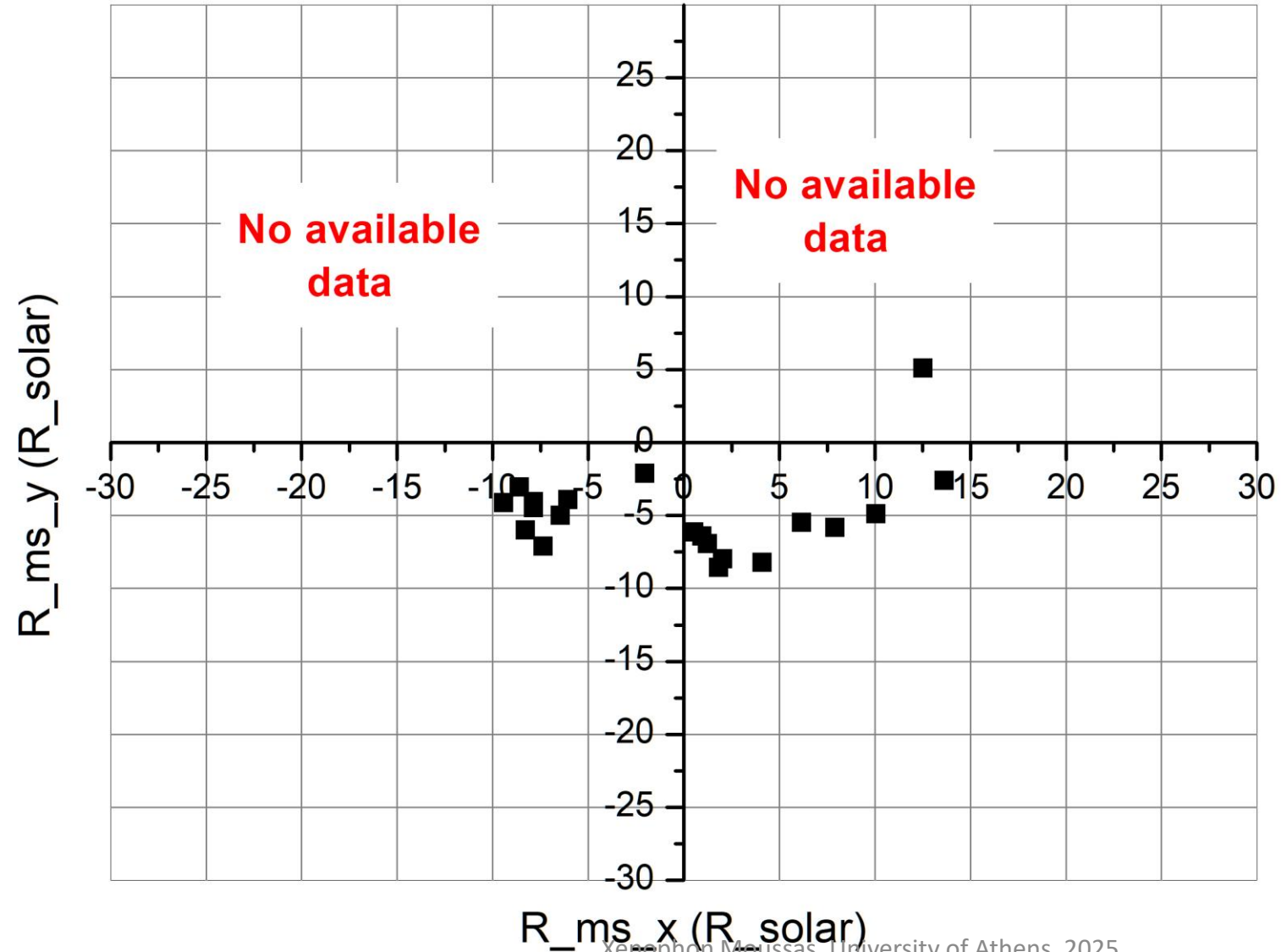
2 days average data from PSP hourly averages
(2019 D:92 - 2019 D:239, 1 rotation around Sun)

■ Solar Wind Magnetosonic Radius (in Solar radii) - Equatorial plane



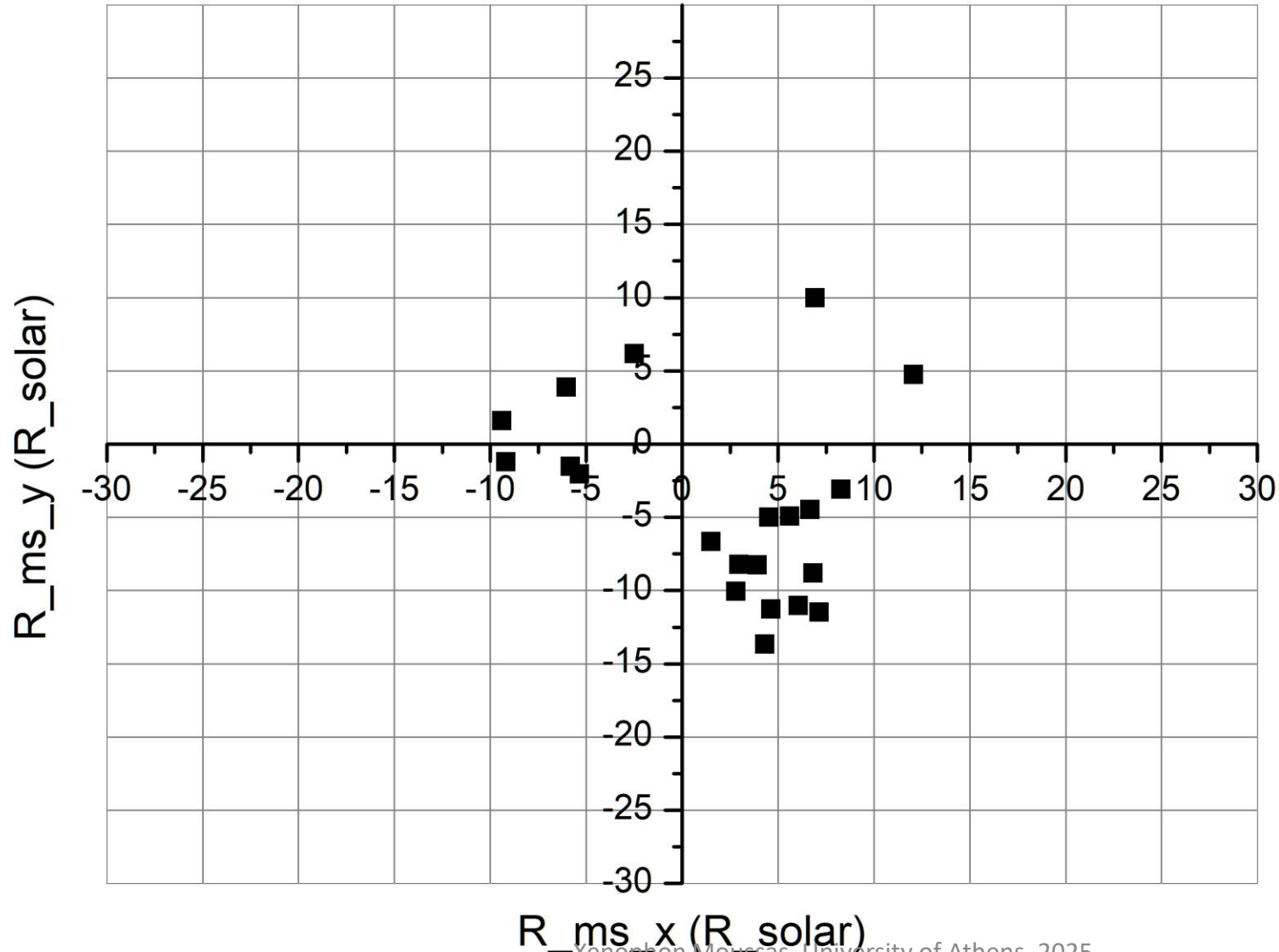
2 days average data from PSP hourly averages
(2019 D:242 - 2020 D:24, 1 rotation around Sun)

■ Solar Wind Magnetosonic Radius (in Solar radii) - Equatorial plane



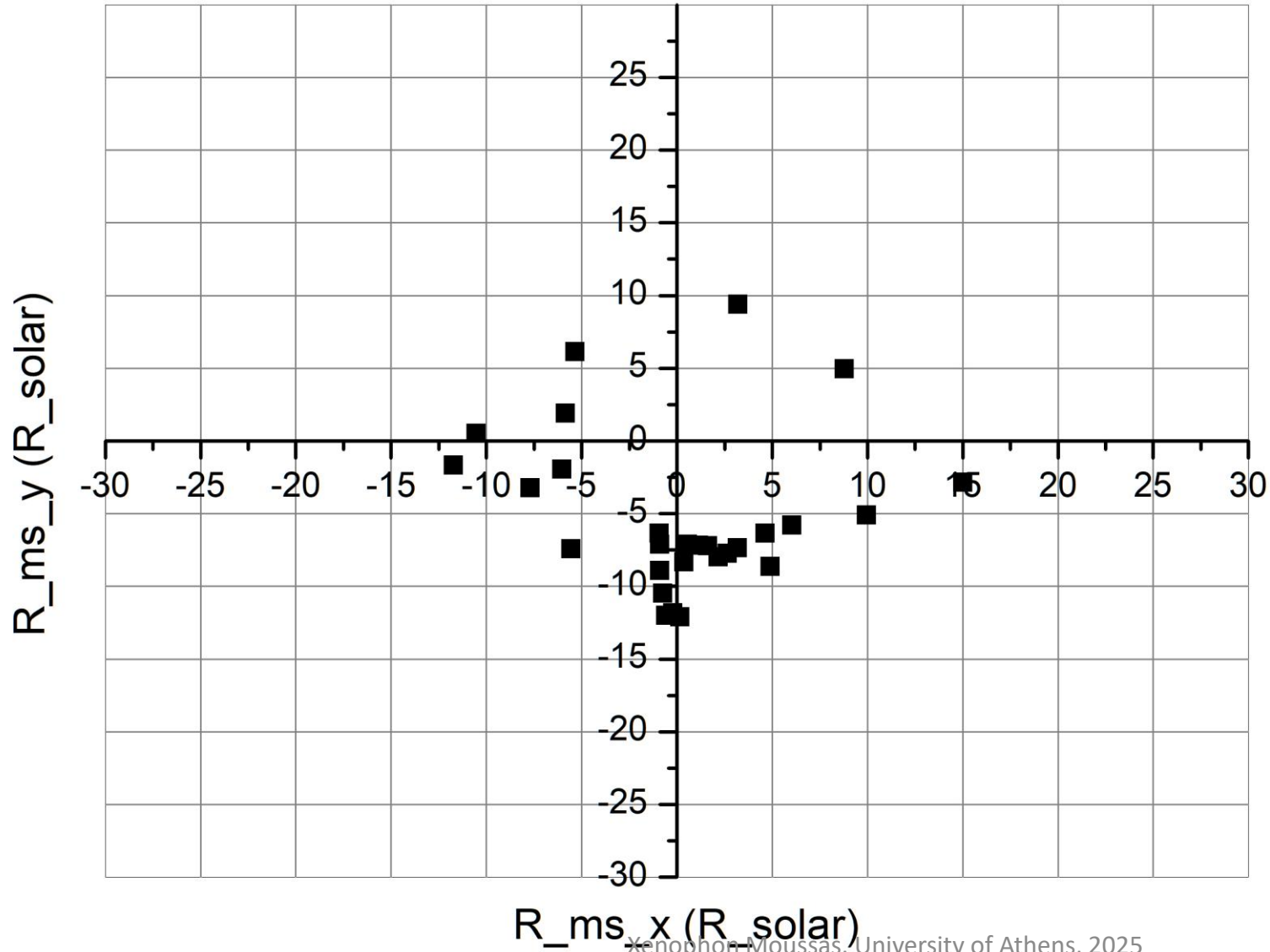
2 days average data from PSP hourly averages
(2020 D:26 - 2020 D:153, 1 rotation around Sun)

■ Solar Wind Magnetosonic Radius (in Solar radii) - Equatorial plane



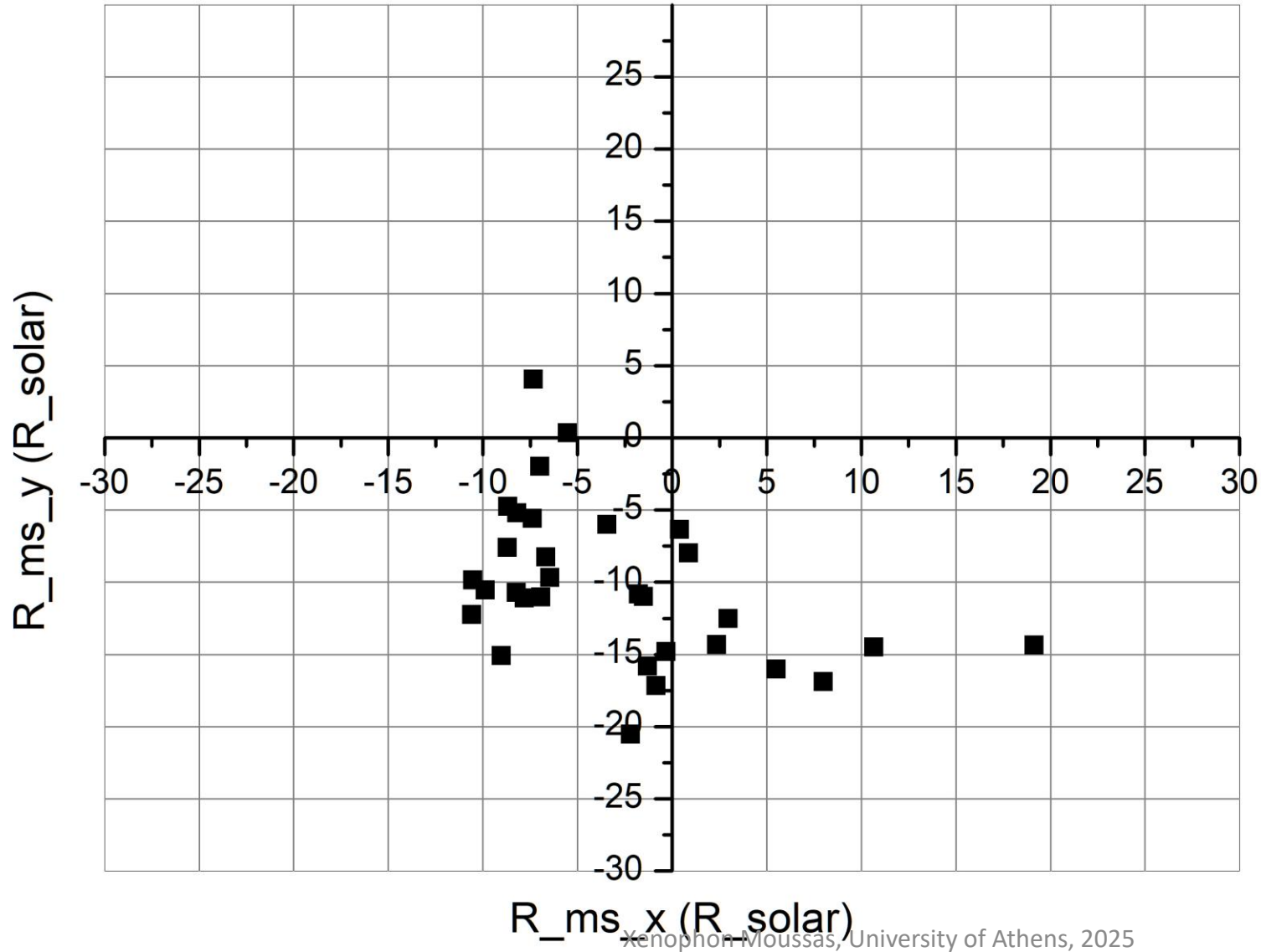
2 days average data from PSP hourly averages
(2020 D:157 - 2020 D:270, 1 rotation around Sun)

■ Solar Wind Magnetosonic Radius (in Solar radii) - Equatorial plane



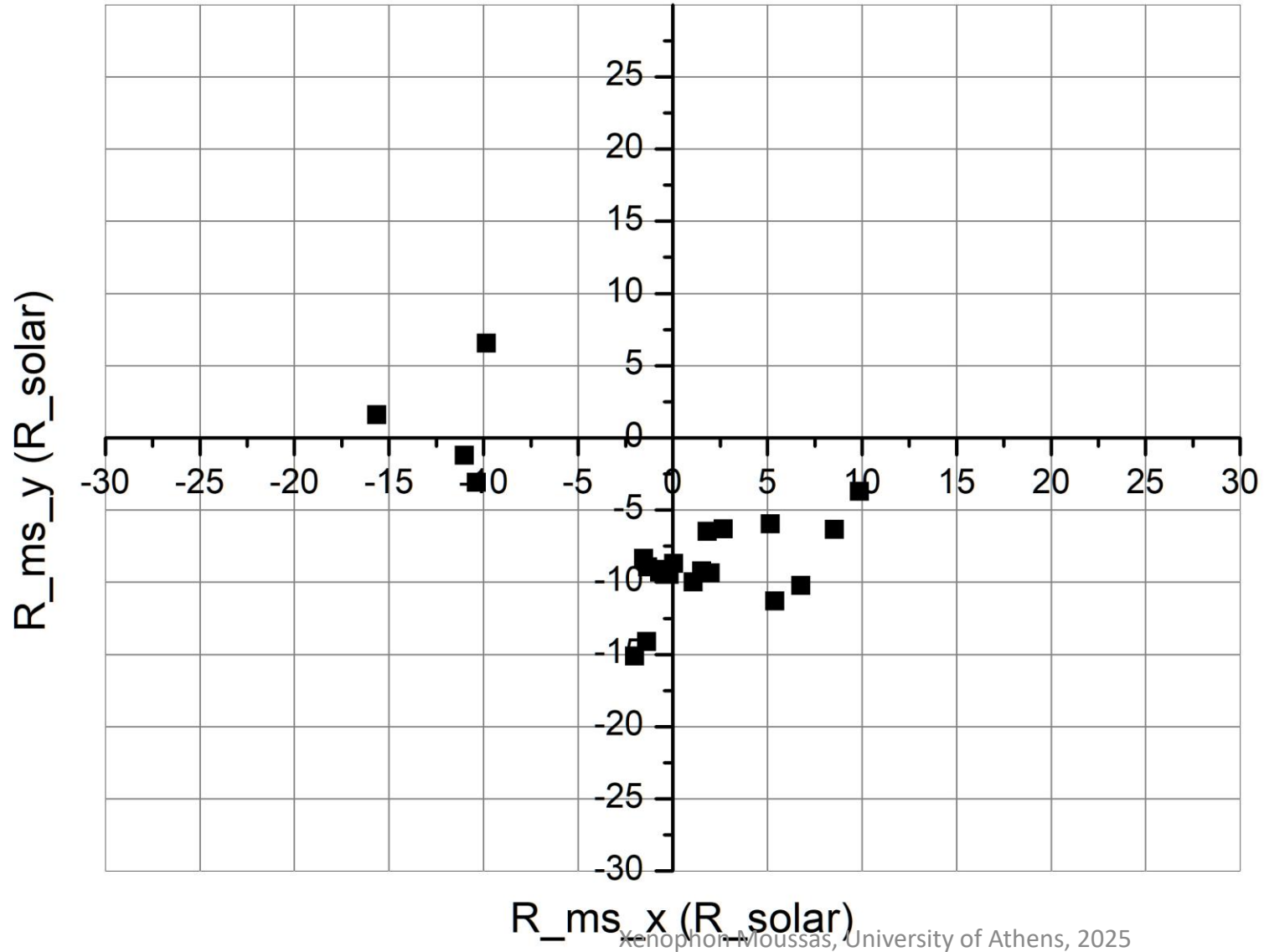
2 days average data from PSP hourly averages
(2022 D:57 - 2022 D:150, 1 rotation around Sun)

■ Solar Wind Magnetosonic Radius (in Solar radii) - Equatorial plane



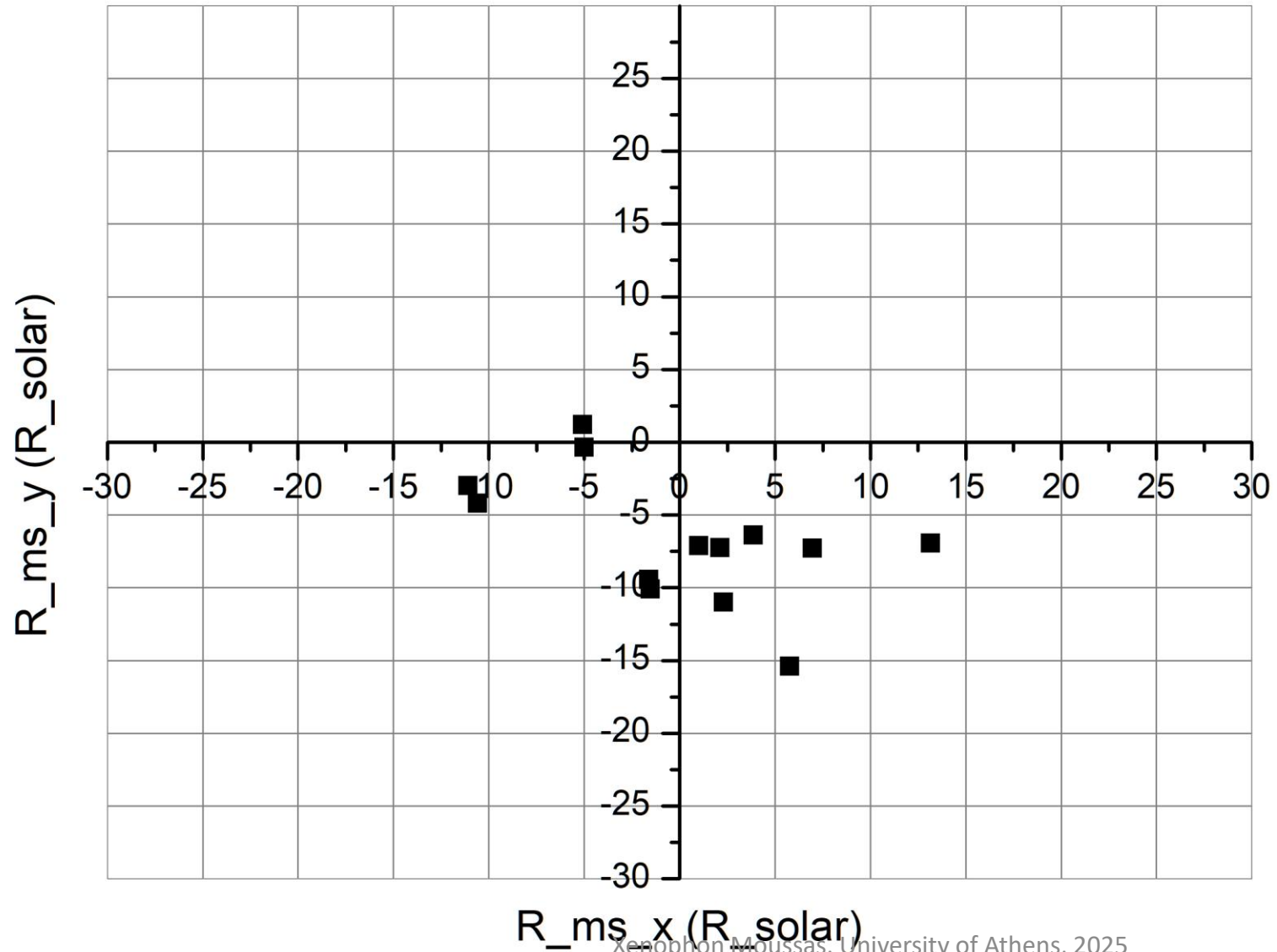
2 days average data from PSP hourly averages
(2020 D:273 - 2021 D:14, 1 rotation around Sun)

■ Solar Wind Magnetosonic Radius (in Solar radii) - Equatorial plane



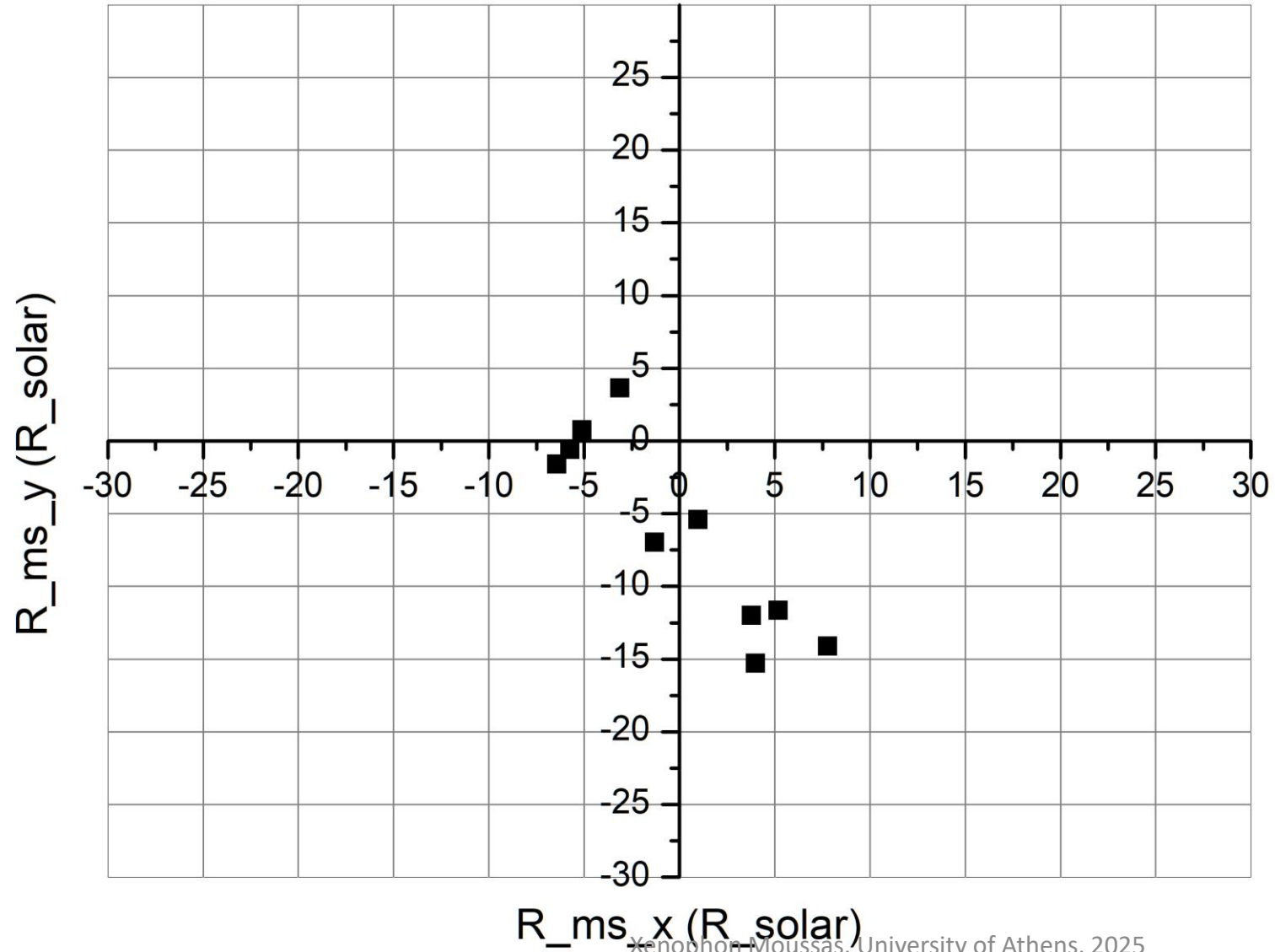
2 days average data from PSP hourly averages
(2021 D:22 - 2021 D:117, 1 rotation around Sun)

■ Solar Wind Magnetosonic Radius (in Solar radii) - Equatorial plane



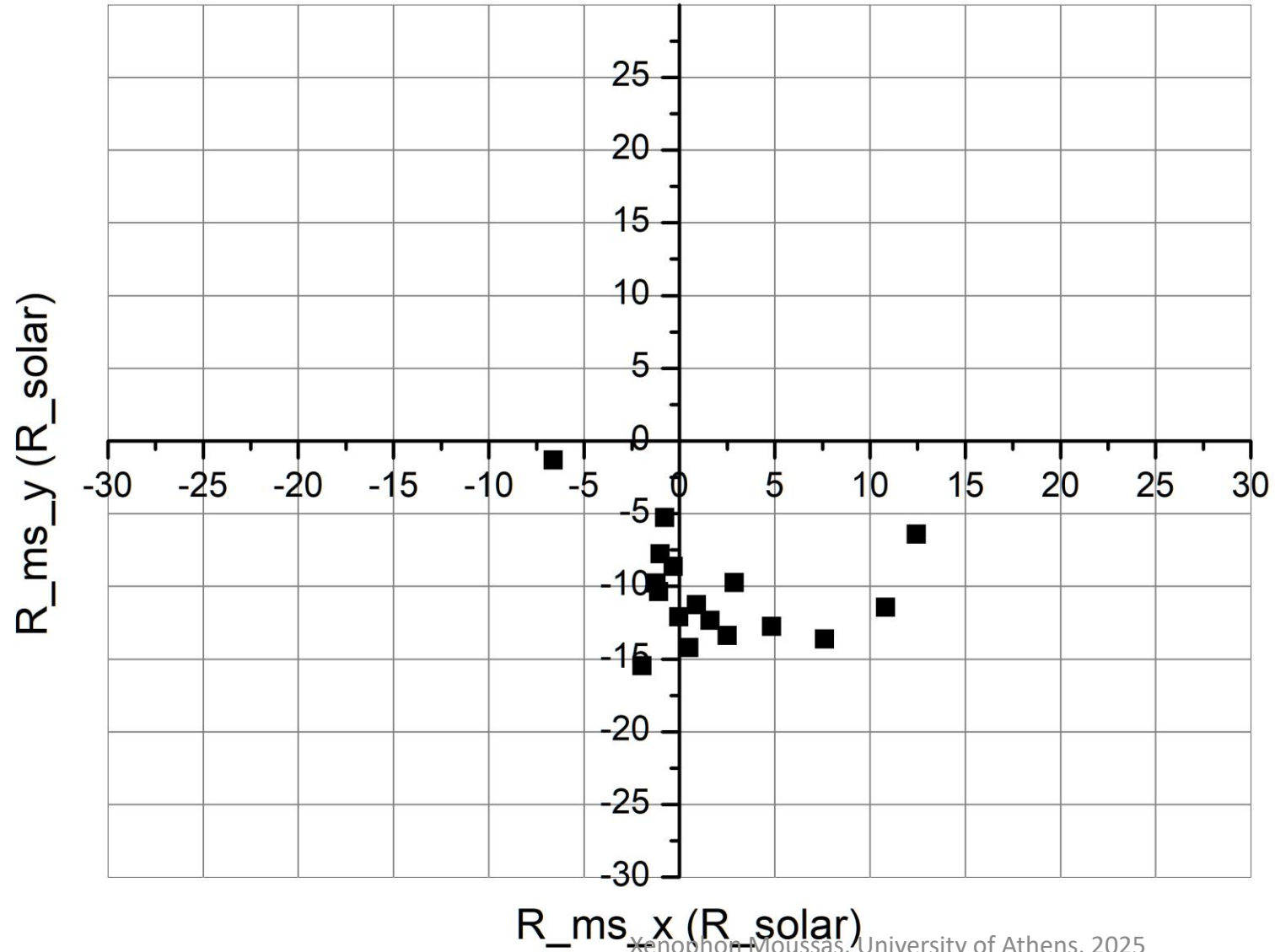
2 days average data from PSP hourly averages
(2021 D:120 - 2021 D:216, 1 rotation around Sun)

- Solar Wind Magnetosonic Radius (in Solar radii) - Equatorial plane



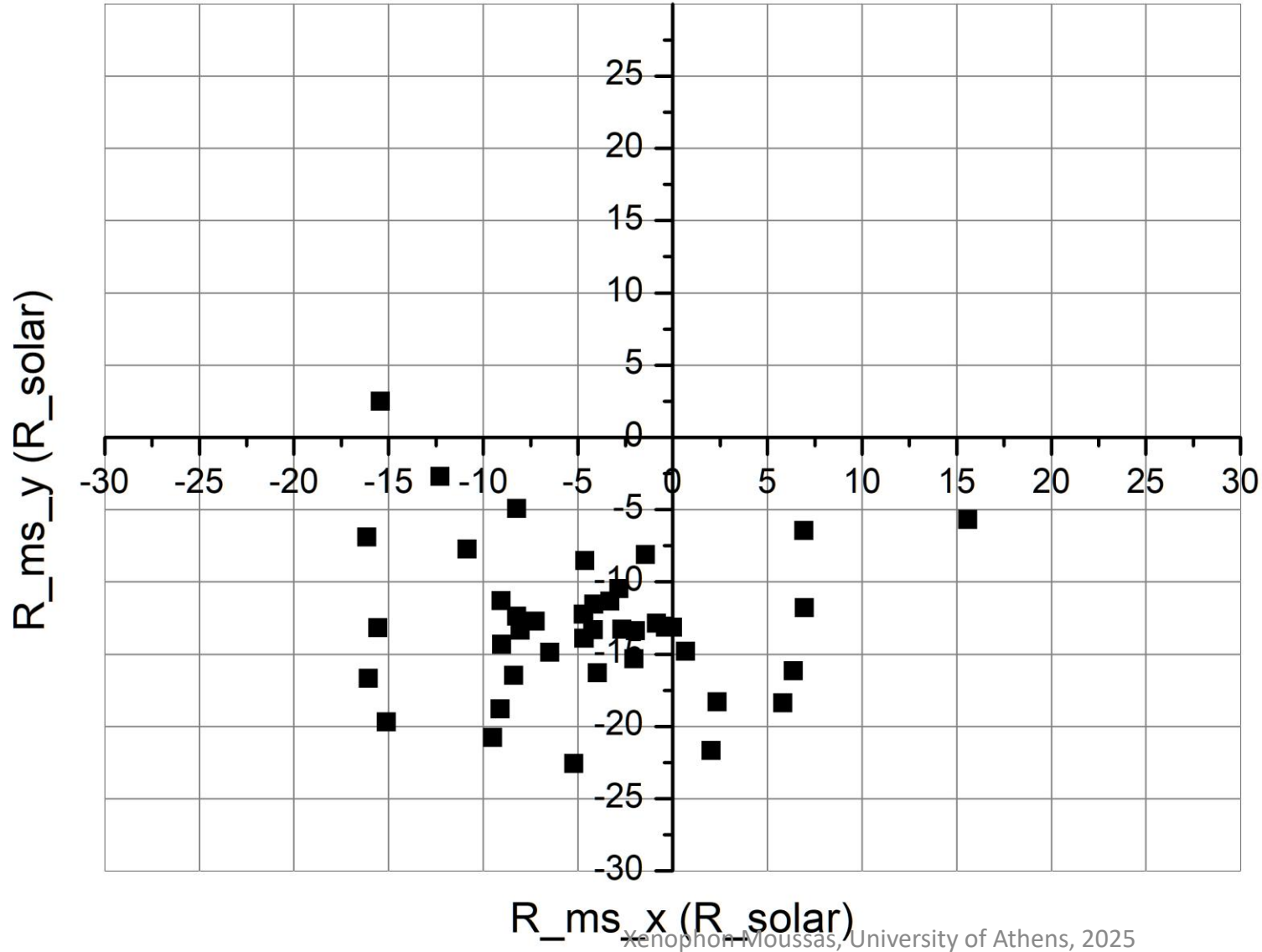
2 days average data from PSP hourly averages
(2021 D:227 - 2022 D:55, 1 rotation around Sun)

- Solar Wind Magnetosonic Radius (in Solar radii) - Equatorial plane



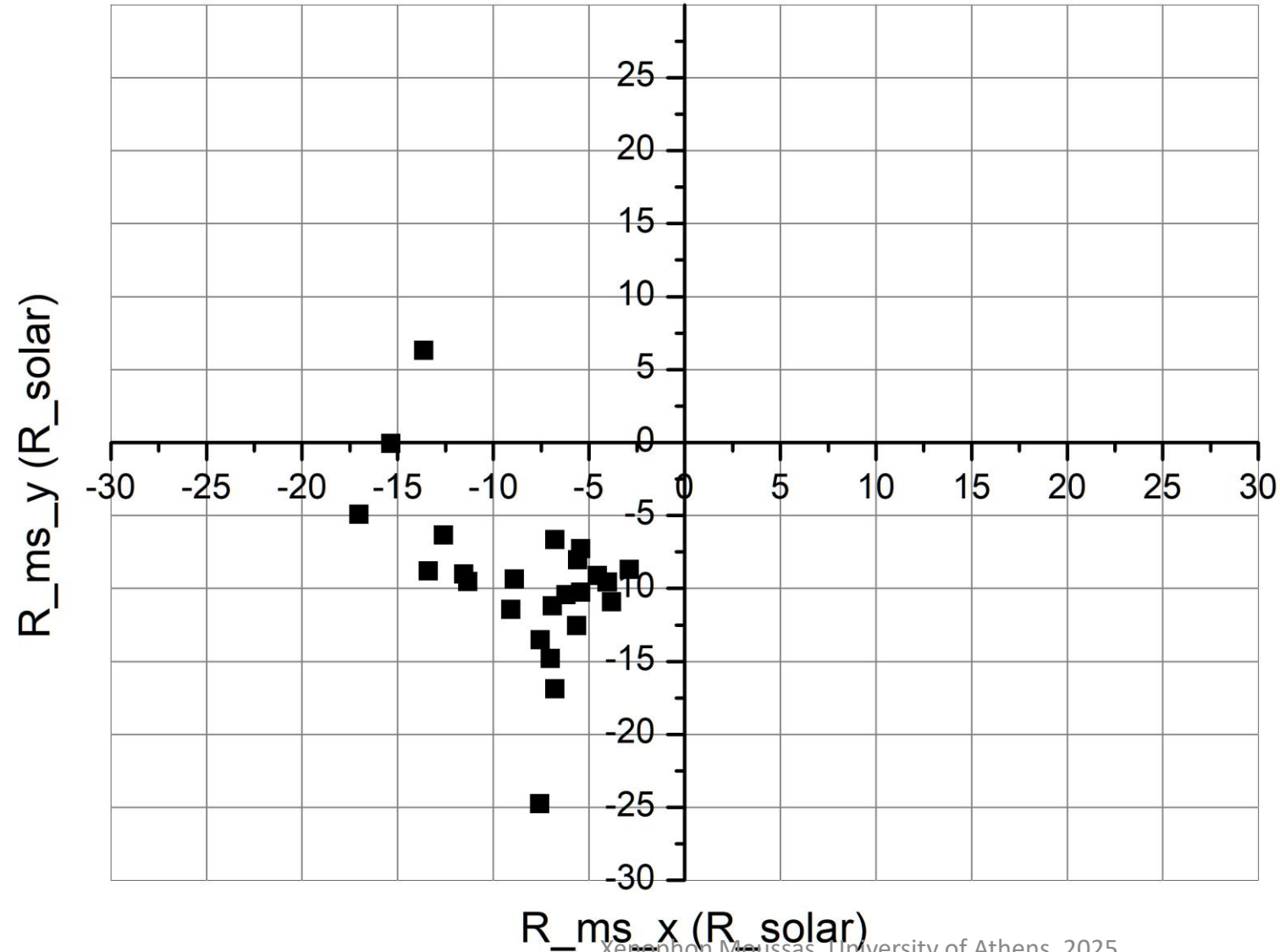
2 days average data from PSP hourly averages
(2022 D:155 - 2022 D:248, 1 rotation around Sun)

■ Solar Wind Magnetosonic Radius (in Solar radii) - Equatorial plane



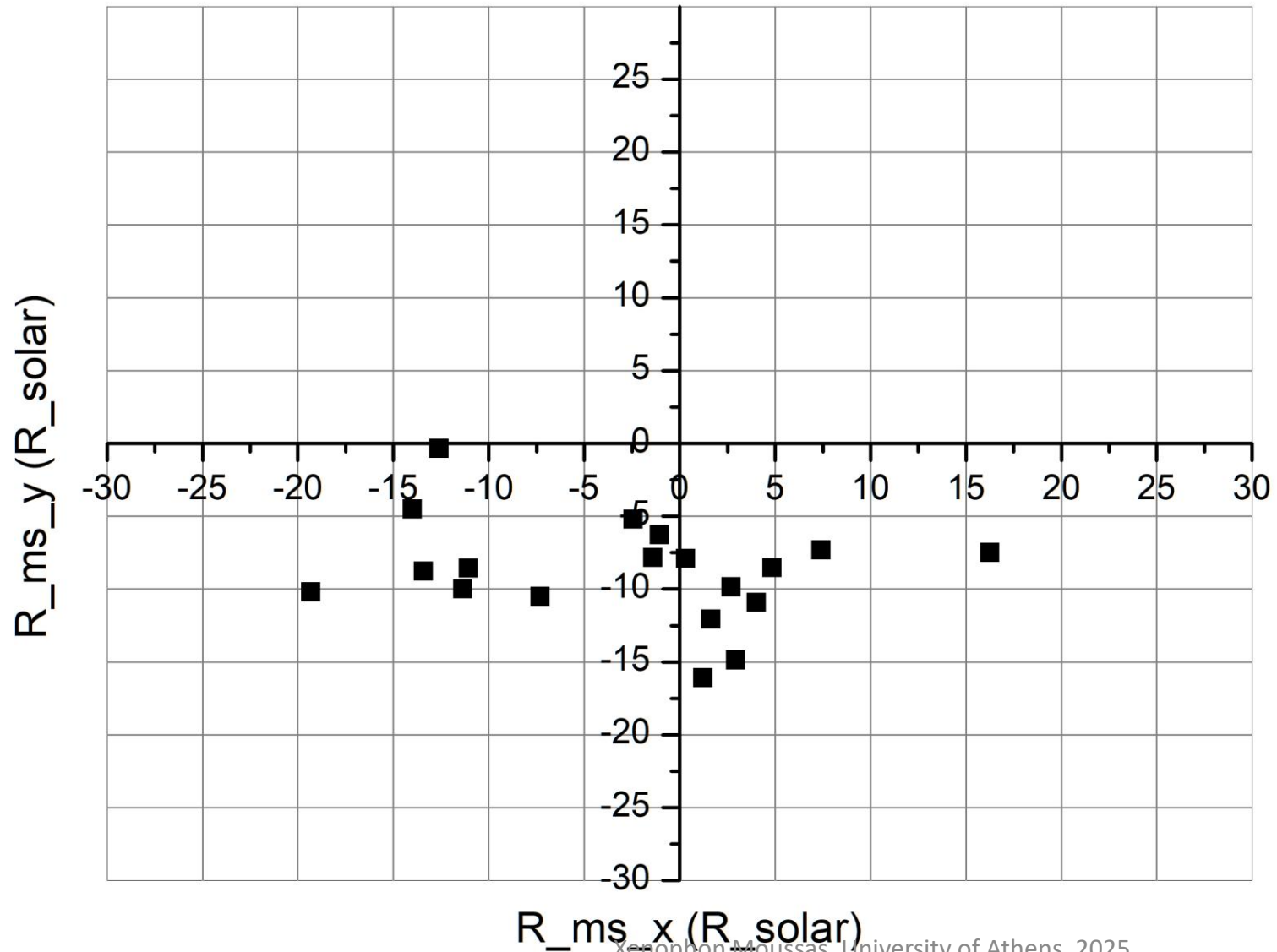
2 days average data from PSP hourly averages
(2022 D:250 - 2022 D:302, 1 rotation around Sun)

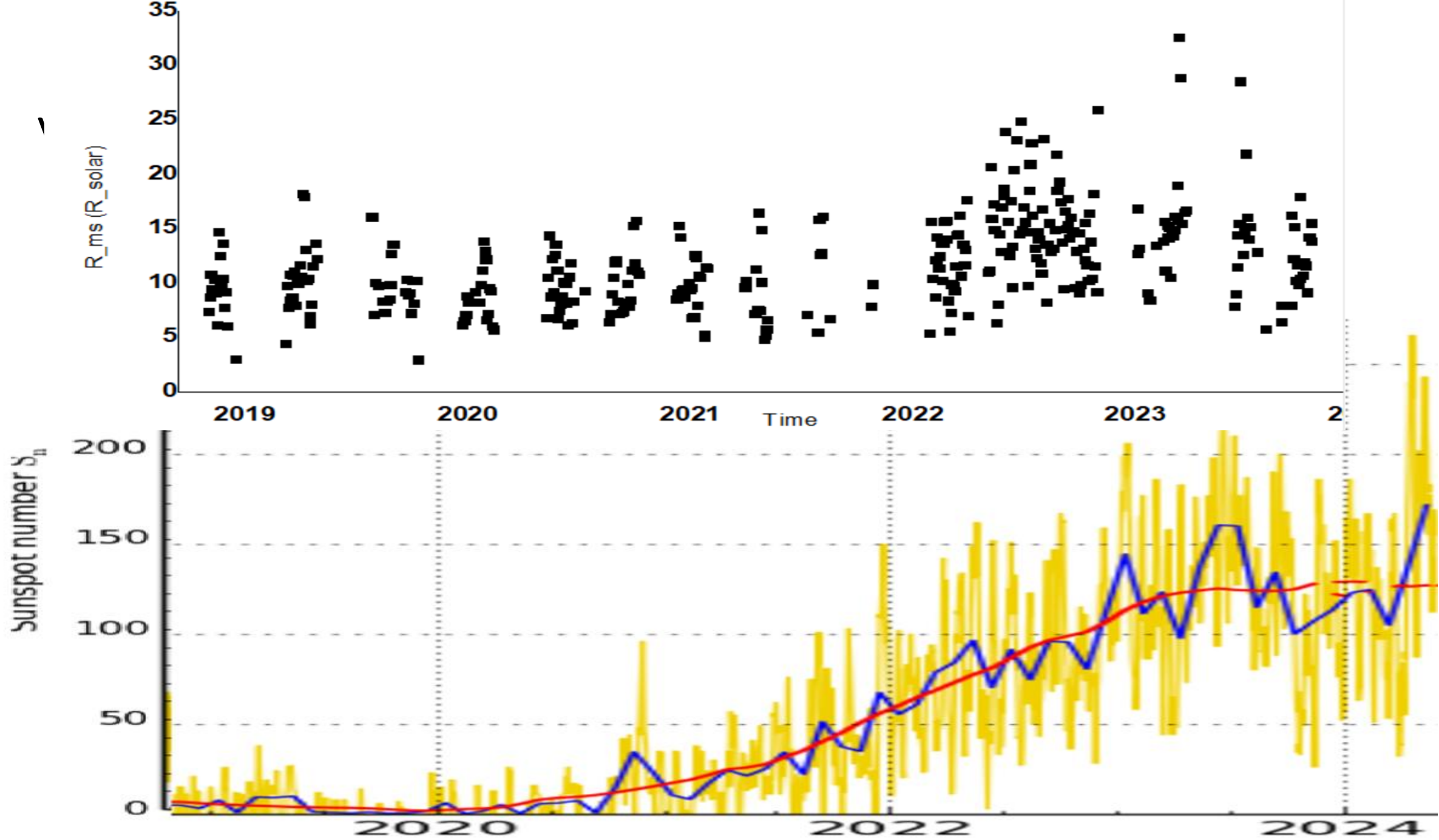
■ Solar Wind Magnetosonic Radius (in Solar radii) - Equatorial plane



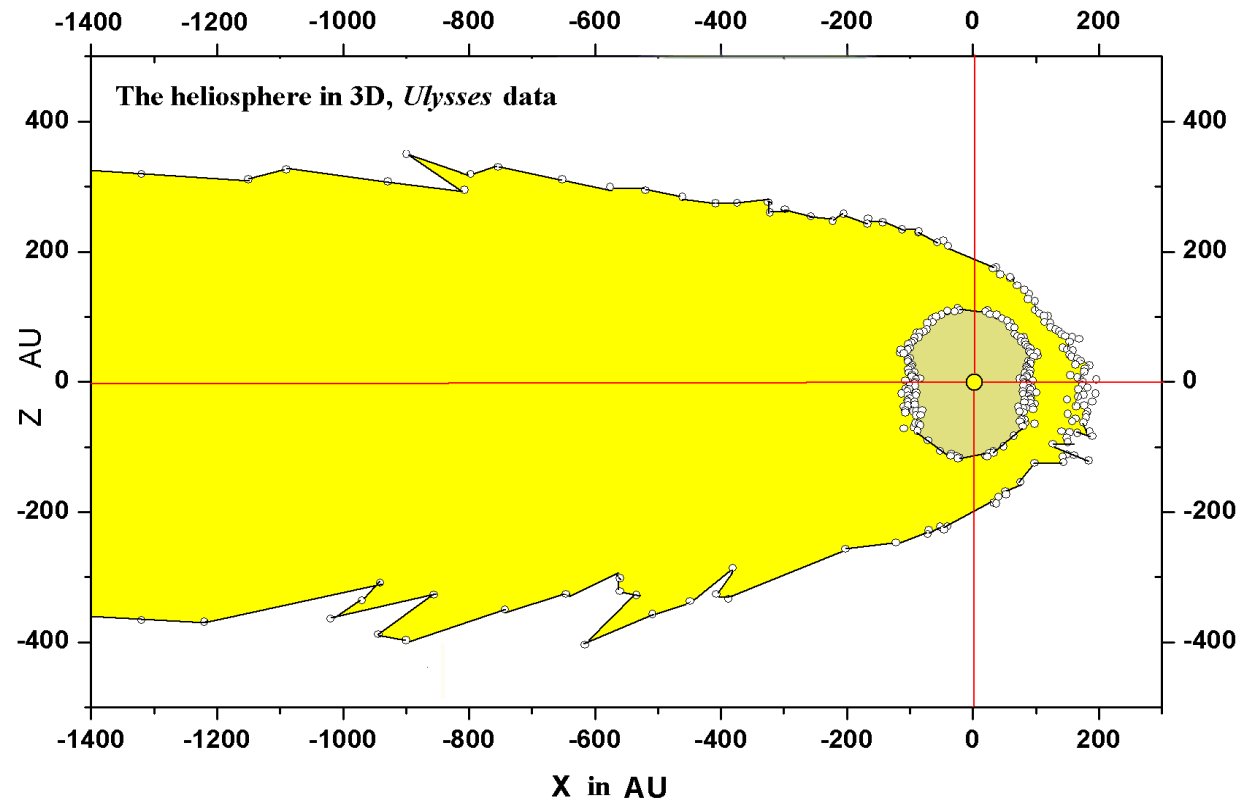
2 days average data from PSP hourly averages
(2023 D:176 - 2023 D:270, 1 rotation around Sun)

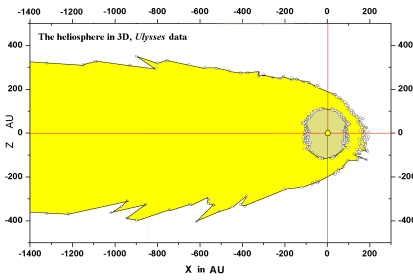
■ Solar Wind Magnetosonic Radius (in Solar radii) - Equatorial plane





appendix





THE LOCATION OF THE HELIOSPHERIC TERMINATION SHOCK



2.1. Analysis

From Rankine-Hugoniot shock jump conditions for a strong oblique termination shock, we get (Barnes 1998)

$$u_s \sin \beta = u_1 \sin \alpha \quad (1)$$

$$u_s \cos \beta = \left(\frac{\gamma - 1}{\gamma + 1} \right) u_1 \cos \alpha \quad (2)$$

$$\rho_s = \rho_1 \left(\frac{\gamma + 1}{\gamma - 1} \right) \quad (3)$$

$$p_s = \rho_1 u_1^2 \left(\frac{2}{\gamma + 1} \right) \cos^2 \alpha, \quad (4)$$

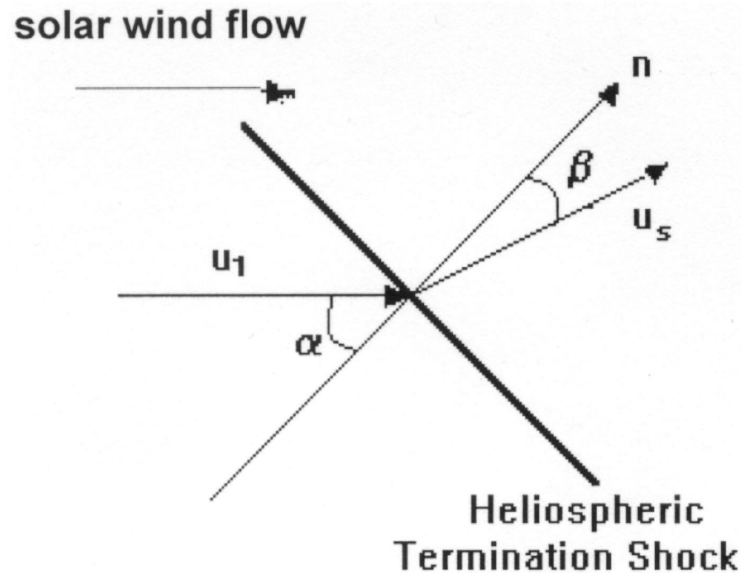
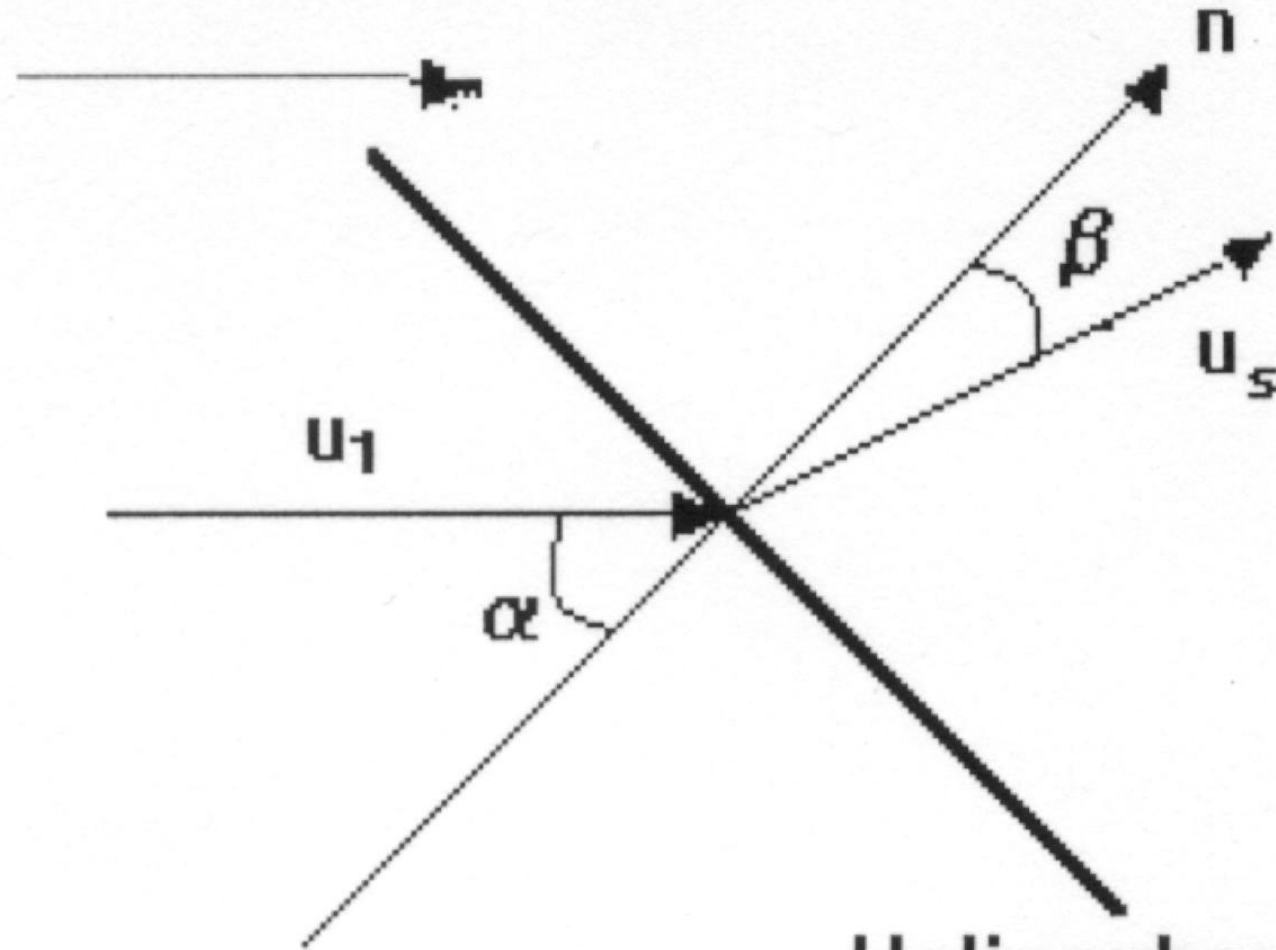


FIG. 1.—Solar wind passing through an oblique termination shock



solar wind flow



Heliospheric
Termination Shock

FIG. 1.—Solar wind passing through an oblique termination shock



Then equation (4), with the help of equations (2) and (5), becomes

$$p_s = \rho_1 u_1^2 \frac{2(\gamma + 1)}{(\gamma - 1)^2} \frac{\cos^2 \beta}{[4\gamma/(\gamma - 1)^2] \cos^2 \beta + 1} . \quad (6)$$

The pressure distribution p_s on the termination shock is obtained applying the Bernoulli equation for the flow between the termination shock and the heliopause, assuming that the flow is incompressible (see § 1):

$$\frac{1}{2}\rho_s u_s^2 + p_s = \frac{1}{2}\rho_\infty u_\infty^2 + p_\infty . \quad (7)$$

Substituting ρ_s from equation (3) and u_s from equation (5) and then solving for p_s , we take

$$p_s = p_\infty + \frac{1}{2} \rho_\infty u_\infty^2 - \frac{1}{2} \rho_1 \left(\frac{\gamma + 1}{\gamma - 1} \right) \times \frac{u_1^2}{[4\gamma/(\gamma - 1)^2] \cos^2 \beta + 1} . \quad (8)$$



The solar wind density ρ_1 upstream of the termination shock varies with radial distance r like

$$\rho_1 = \rho_o \left(\frac{r_o}{r_s} \right)^2, \quad (9)$$

$$\left(\frac{r_s}{r_o} \right)^2 = \frac{\rho_o(\gamma + 1) \{ u_1^2 + [u_s^2 / (\gamma - 1)] \}}{2\gamma(p_\infty + \frac{1}{2}\rho_\infty u_\infty^2)}.$$



We express the **velocity potential of the flow after the termination shock** in the form (**Fahr et al. 1993; Nerney & Suess 1995**)

where P are the associated Legendre polynomials

$$\Phi = \sum_{lm} (A_{lm} r^l + B_{lm} r^{-(l+1)}) \cos m\phi P_l^m(\cos \theta)$$

$$\Phi = A_o + \frac{B_o}{r} + r(A \cos \phi \sin \theta + B \cos \theta) + \frac{1}{r^2} (\Gamma \cos \phi \sin \theta + \Delta \cos \theta)$$

$$u_r = -\frac{\partial \Phi}{\partial r} = \frac{B_o}{r^2} - (A \cos \theta \sin \theta + B \cos \theta) + \frac{2}{r^3} (\Gamma \cos \phi \sin \theta + \Delta \cos \theta)$$

$$u_\theta = -\frac{1}{r} \frac{\partial \Phi}{\partial \theta} = -A \cos \phi \cos \theta + B \sin \theta - \frac{1}{r^3} (\Gamma \cos \phi \cos \theta - \Delta \sin \theta)$$

$$u_\phi = -\frac{1}{r \sin \theta} \frac{\partial \Phi}{\partial \phi} = A \sin \phi + \frac{\Gamma \sin \phi}{r^3} .$$

The boundary conditions that we use are the following:

1. $\mathbf{u}(r \rightarrow \infty) = -u_\infty \hat{\mathbf{z}}$;
2. $r_s(\theta = \pi/2, \phi = 0) = r_s(\theta = \pi/2, \phi = \pi)$;
3. $u(r = r_{hp}, \theta = 0) = 0$;
4. $u[r = r_s(\theta = 0)] = (\gamma - 1)/(\gamma + 1)u_1$.

From condition 2 we find that $A = 0$ and $\Gamma = 0$.

From condition 1

$$B = u_\infty .$$

From condition 3 we have $B_o = \left[B - \frac{2\Delta}{r_h^3(\theta = 0)} \right] r_h^2(\theta = 0)$

$$\Delta = \frac{\{[(\gamma - 1)/(\gamma + 1)]u_1 + u_\infty\}r_s^2(\theta = 0) - u_\infty^2 r_h^2(\theta = 0)}{2\{[1/r_s(\theta = 0)] - [1/r_h(\theta = 0)]\}} .$$

the only unknown parameters are
the termination shock radius
and the heliopause radius $r_s r_h$

$r_s(0)$ can be determined from:

$$\left(\frac{r_s}{r_o}\right)^2 = \frac{\rho_o(\gamma + 1)\{u_1^2 + [u_s^2/(\gamma - 1)]\}}{2\gamma(p_\infty + \frac{1}{2}\rho_\infty u_\infty^2)} .$$

$r_h(0)$ can be determined from the one-dimensional model by
Khabibrakhmanov et al. 1996)

$$r_h(0) - r_s(0) = 37.6 \text{ AU} .$$

CR modulation

$$J = J_o \exp(-\gamma u_{sw} B^\alpha)$$

$$\begin{aligned} J(i, j) = & \left(J(i-1, j) \exp(-\gamma_1 u_{sw} B_{(i-1, j)}^\alpha) \right. \\ & + J(i-1, j-1) \exp(\gamma_2 u_{sw} B_{(i-1, j-1)}^\alpha) \\ & \left. + J(i-1, j+1) \exp(-\gamma_3 u_{sw} B_{(i-1, j+1)}^\alpha) \right) / 3.0, \end{aligned}$$